Pyrene-Labeled Poly(aryl ether) Monodendrons: Synthesis, Characterization, Diffusion Coefficients, and Photophysical Studies

Jeanne M. Riley,[†] Sibel Alkan,[†] Aidi Chen,[‡] Michael Shapiro,*[,‡,§] Wajiha A. Khan,[†] W. Rorer Murphy, Jr.,[†] and James E. Hanson*[,†]

Department of Chemistry, Seton Hall University, 400 South Orange Avenue, South Orange, New Jersey 07079-2694, and Novartis Pharmaceuticals Corporation, 556 Morris Avenue, Summit, New Jersey 07901-1398

Received May 8, 2000; Revised Manuscript Received November 30, 2000

ABSTRACT: Four generations of poly(aryl ether) monodendrons labeled with pyrene at the focus were synthesized and characterized by a combination of NMR, size-exclusion chromatography with light scattering detection, and electronic spectroscopy. The monodendrons were then studied by magnetic resonance and fluorescence techniques. Translational diffusion coefficients in THF-d_8, acetonitrile-d_3, and cyclohexane-d_{12} were measured by pulsed-field-gradient NMR and ranged from 2.2×10^{-5} cm^2/s for methoxypyrene in acetonitrile to 3.4×10^{-6} cm^2/s for the fourth generation monodendron in THF. Molecular radii were calculated from the diffusion coefficients by the Stokes−Einstein equation. In THF, the radii increased from 2.8 Å for methoxypyrene to 14 Å for the fourth generation monodendron. In acetonitrile the radii were smaller, increasing from 2.7 Å for methoxypyrene to 5.4 Å for the third generation monodendron. In both solvents, a change in solution structure between the second and third generation monodendrons was observed in the diffusion data. The rate of fluorescence quenching by molecular oxygen was measured for the pyrene-labeled monodendrons in THF, acetonitrile, and cyclohexane and was found to decrease for monodendrons of increasing generation. This decrease cannot be fully explained by the slower diffusion of the larger monodendrons. Several simple models for the reduced quenching rate of the pyrene chromophore were developed. These models suggest that the increased density of the larger monodendrons provides a more effective barrier to diffusing dioxygen.

Dendritic polymers (dendrimers) have been the subject of considerable recent interest,[1] and many details of their solution structure remain an open question. Most dendrimers are flexible molecules with numerous low-energy conformations, so the structure and size of these molecules in solution have been debated. The early model of de Gennes[2] assumed fully extended structures, with a "dense packed" state for molecules where the surface groups exceeded the available surface area. Recent theoretical work[3] has suggested some backfolding of the branches, resulting in sizes reduced from full extension. These results imply open structures for smaller dendritic molecules, while larger molecules should have more spherical shapes and denser packing.[3] We have begun a series of experimental investigations designed to probe the structure and dynamics of dendrimers and report the results of magnetic resonance and fluorescence studies of pyrene-labeled poly(aryl ether) monodendrons.

Attempts have been made to verify the theoretical models experimentally using a variety of physical methods, including magnetic resonance[4] and fluorescence methods.[5] A selection of these studies relevant to our work is summarized here. Solution radii of dendritic polymers have been studied previously. Mourey, Frechet, and co-workers measured the solution viscosity of poly(aryl ether) dendrimers in THF.[6] The intrinsic viscosity for monodendrons increased up to generation 5 (G5), then decreased for G6. Calculated hydrodynamic radii increased from 8 Å for G2 to 22 Å for G6. Hult used pulsed-field spin−echo NMR to determine diffusion coefficients (D) for aliphatic polyester dendrimers in $CDCl_3$ at 298 K.[4] Values for D decreased with increasing generation, from 5.12×10^{-6} cm^2/s for G1 (MW = 906) to 2.36×10^{-6} cm^2/s for G4 (MW = 7549). Radii determined from the Stokes−Einstein relation increased from 7.8 Å for G1 to 17.1 Å for G4. DeSchryver used fluorescence depolarization to measure hydrodynamic volumes of poly(aryl ether) didendrons with a rubicene core.[5a] In toluene, the hydrodynamic volume increased from 4030 Å^3 for G1 (MW = 962) to 18 850 Å^3 for G4 (MW = 6898). In acetonitrile, a poorer solvent, the volume increased from G1 (3230 Å^3) to G3 (9730 Å^3, MW = 3506) and then decreased to 6490 Å^3 for G4.

Photophysical methods have also been applied to dendritic polymers. Frechet measured the solvatochromism of poly(aryl ether) monodendrons with a nitroaniline group at the focus.[5b] The absorbance λ_{max} moved to longer wavelengths from G0 to G6, with larger shifts in nonpolar solvents and the largest shift between generations 3 and 4. Gauthier et al studied fluorescence quenching of pyrene-labeled arborescent polystyrenes.[5c] Stern−Volmer analysis suggested that some fluorophores were inaccessible to the quencher. The sum of the diffusion coefficients for fluorophore and quencher decreased with increasing generation, and it was concluded that the arborescent polymers had higher segmental density and fewer accessible chromophores than linear polymers. Metalloporphyrins surrounded by poly(aryl ether) monodendrons have been studied by Frechet and Abruna[5d] and also by Aida,[5e] with interesting results on site isolation from electrochemical and photochemical measurements. Vitukhnovsky et al.[5f] reported fluorescence quenching and excimer formation for pyrene-labeled polyallylcarbosilane monodendrons

[†] Seton Hall University.
[‡] Novartis Pharmaceuticals Corporation.
[§] Present address: Lilly Research Laboratories, Lilly Corporate Center, Indianapolis, IN 46285.

10.1021/ma0007886 CCC: $20.00
Published on Web 02/10/2001

and hyperbranched polymers. Diffusion coefficients extracted from the quenching data were found to be similar for monodendrons and hyperbranched polymers of approximately equal molecular weight.

At the time of the publications by Hult[4] and DeSchryver,[5a] we had initiated the NMR determination of the diffusion coefficients for a series of poly(aryl ether) monodendrons labeled with pyrene at the focus.[7] This study was begun to aid in the interpretation of extensive photophysical characterization of these molecules. We report here the use of a pulsed field gradient NMR technique[8] to determine the diffusion coefficients for a series of monodendrons labeled with pyrene at the focus and also the measurement of fluorescence quenching by oxygen for these molecules. The diffusion coefficients allow calculation of the molecular sizes of the monodendrons, and the diffusion data facilitate the interpretation of the quenching measurements to provide deeper insights into the solution structure of these monodendrons.

Experimental Section

General. Melting points were determined on a Mel-Temp apparatus and are uncorrected. Tetrahydrofuran (THF) was purified by distillation from sodium/benzophenone immediately before use as a reaction solvent. Except where noted, all other chemicals were purchased from commercial vendors and used without further purification. ^{1}H NMR spectra were recorded in acetone-d_6 or $CDCl_3$ on a General Electric QE-300 FT-NMR or a Varian XL-400 FT-NMR and are given in δ units based on an internal tetramethylsilane (TMS) reference. ^{13}C NMR spectra were recorded in $CDCl_3$ on a Varian 200 MHz FT-NMR and are given in ppm units based on a TMS reference. For NMR data the following abbreviations are used: Ar refers to protons on an aromatic ring of the dendritic structures and the subscript refers to the generation of the ring. The terminal aromatic rings are assigned the number 0 (i.e., Ar_0) and the numbers increase "upward" through a dendritic structure of generation n until the unique aromatic ring at the focus is assigned the number n (Ar_n). Ar′ refers to the aromatic rings of the core pyrene molecule. Analytical thin-layer chromatography was performed on commercially coated silica gel plates (200−400 mesh, 60 Å). Silica gel for flash chromatography was 200−400 mesh, 60 Å. Elemental analyses were performed by Schwartzkopf Microanalytical Laboratories, Woodside, NY.

Size Exclusion Chromatography. Size exclusion chromatography was performed with a Waters 510 pump, Waters 078700 in-line degasser, a Polymer Laboratories PLGel 5μ 500 Å column with guard column, Precision Detectors light scattering detector, and a Waters 410 refractive index detector. The eluent for all size exclusion chromatography (SEC) analysis was inhibitor-free THF, and flow rates were between 1.0 and 1.5 mL/min. The system was calibrated using polystyrene standards from Polymer Laboratories.

Electrochemistry. Electrochemical experiments were performed on a BAS C-50W electrochemical analyzer with a CV-2 Faraday cage cell stand. All measurements were made in spectral grade methylene chloride with 0.1 M tetrabutylammonium hexafluorophosphate (TBAH) as the supporting electrolyte. The TBAH was recrystallized twice before use. For cyclic voltammetry, a platinum disk working electrode, a platinum wire auxiliary electrode, and a 3 M NaCl Ag/AgCl reference electrode (+0.20 V vs the normal hydrogen electrode) were used. All cyclic voltammograms were run at a scan rate of 100 mV/s.

Photophysical Measurements. Solvents for spectroscopy were HPLC grade and were obtained from commercial suppliers. Compressed air, oxygen, and argon were obtained from commercial suppliers. UV−vis spectra were collected using a Hewlett-Packard 8540A photodiode array spectrophotometer. UV quartz fluorescence cells (Spectrosil) were purchased from Starna. Emission and lifetime measurements were performed on a Jobin-Yvon Spex Tau-2 (FL1T11) spectrofluorimeter consisting of a 450-W xenon lamp, a single grating excitation monochromator, a removable Pockels cell for frequency modulation, a single grating emission monochromator, and a T-box sampling module. All spectra were measured at 25 °C at right angle and collected on a Hamamatsu R928 photomultiplier tube. Emission spectra were corrected for detector response by an internal Rhodamine B quantum counter and correction files. Native lifetimes τ_o were determined from solutions which had been deoxygenated by a minimum of three freeze−pump−thaw cycles. Quenched lifetimes τ were determined from solutions saturated by bubbling with either air or oxygen for a minimum of 15 min. Lifetime measurements were obtained by the frequency-modulation technique.[9] The excitation wavelength was 332 nm and scattered light was rejected by a colored glass filter (<0.5% transmission at ≤335 nm, Kopp Glass #7380). Data were acquired at 15 frequencies between 3.0 and 40.0 MHz.. Lifetimes were evaluated using Globals Unlimited software from the Laboratory for Fluorescence Dynamics at the University of Illinois at Urbana-Champaign. All lifetime data were well described by a monoexponential model, with goodness of fit parameter $\chi_R^2 < 1.2$.

Gradient NMR Measurements. Measurements were made on a Bruker DMX-500 NMR with a 5-mm inverse broad band probe with triple axis gradients or a Bruker DMX-400 NMR with a 5-mm inverse broad band z-gradient probe using the bipolar LED sequence developed by Wu et al.[8] The diffusion coefficients were obtained from linear regression analysis of the natural logarithm of the intensity as a function of the gradient strength squared. Diffusion coefficients of the solvent (THF, acetonitrile, or cyclohexane) and adventitious water were used as internal standards.

Synthesis. Synthetic details and characterization data for previously reported procedures can be found in the Supporting Information.

General Procedure for Coupling of (G-*n*) Benzyl Bromides with Methyl 3,5-Dihydroxybenzoate (1).[10,11] Monomer **1** (1.00 equiv) and the appropriate dendritic benzyl bromide (2.00 equiv) were dissolved in dry THF. Anhydrous potassium carbonate (2.5 equiv) and 18-crown-6 (0.20 equiv) were then added. The reaction was refluxed with vigorous stirring under an argon atmosphere for at least 48 h. When the reaction was complete by TLC, the solvent was removed under reduced pressure. The residue was dissolved in methylene chloride and an equal volume of water added. This mixture was extracted three times with methylene chloride, and the organic layers were collected and combined. These were then washed with 10% NaOH solution followed by water. The organic layers were dried over anhydrous sodium sulfate and filtered, and the solvent was removed under reduced pressure. Purification procedures for the individual dendritic esters are provided below.

General Procedure for Reduction of (G-*n*) Methyl Esters to the (G-*n*) Benzyl Alcohols.[12] The appropriate methyl ester (1.00 equiv) was dissolved in dry THF. Lithium chloride (3.00 equiv) and potassium borohydride (3.00 equiv) were slowly added to the solution. The reaction was refluxed with vigorous stirring under argon until the evolution of gas ceased. When the reaction was complete by TLC, the mixture was poured into an equal volume of water to quench the excess borohydride. The mixture was extracted three times with methylene chloride, and the organic layers were collected and combined. These layers were first washed with water and then with saturated aqueous NaCl. The organic layers were dried over sodium sulfate and filtered, and the solvent was removed under reduced pressure. Purification procedures for the individual dendritic alcohols are provided below.

G1CO$_2$CH$_3$ (2). Reaction of benzyl bromide (70.1 mL, 589 mmol) and **1** (45.0 g, 268 mmol) by the general procedure described above for coupling gave **2**. A brown oil was collected that gave a white solid upon recrystallization from diethyl ether. The crystals were collected by filtration and washed with hexanes (to remove excess benzyl bromide) to give **2** (72.7 g, 78%). Mp 60−62 °C. ^{1}H NMR ($CDCl_3$): δ 3.90 (s, 3H, OCH_3),

5.07 (s, 4H, Ar_0CH_2O), 6.80 (t, 1H, Ar_1H), 7.25−7.48 (m, 10H, Ar_0H, 2H, Ar_1H). Size-exclusion chromatography with light scattering detection (SEC-LS): M_w 341 (nominal MW 348), $M_w/M_n = 1.00$. Anal. Calcd for ($C_{22}H_{20}O_4$): C, 75.84, H, 5.79. Found: C, 75.90; H, 5.64.

G1OH (3). Reduction of **2** (58.0 g, 167 mmol) by the general procedure described above for reduction gave **3**. The crude solid was purified by recrystallization from 1:1 (v:v) toluene/cyclohexane. The precipitate was collected by filtration and washed with hexanes giving a white solid (43.7 g, 82%). Mp 66−70 °C. ^{1}H NMR ($CDCl_3$): δ 4.63 (s, 2H, CH_2OH), 5.04 (s, 4H, Ar_0CH_2O), 6.55 (t, 1H, Ar_1H), 6.63 (s, 2H, Ar_1H), 7.25−7.43 (m, 10H, Ar_0H). SEC-LS: M_w 320 (nominal MW 320), $M_w/M_n = 1.00$.

G2CO$_2$CH$_3$ (5). Reaction of G1Br (**4)** (45.0 g, 117 mmol) and **1** (8.97 g, 53 mmol) by the general procedure described above for coupling gave **5**. The crude product was dissolved in a minimal amount of methylene chloride and run through a short column of silica gel. The solution was then concentrated under reduced pressure and the product precipitated into hexanes. A white solid was collected by filtration (35.9 g, 87%). Mp 131−134 °C. ^{1}H NMR ($CDCl_3$): δ 3.91 (s, 3H, OCH_3), 5.00 (s, 4H, Ar_1CH_2O), 5.03 (s, 8H, Ar_0CH_2O), 6.58 (t, 4H, Ar_1H), 6.68 (d, 2H, Ar_1H), 6.76 (t, 1H Ar_2H), 7.25−7.47 (m, 20H, Ar_0H, 2H, Ar_2H). SEC-LS: M_w 697 (nominal MW 773), $M_w/M_n = 1.00$. Anal. Calcd for ($C_{50}H_{44}O_8$): C, 77.70; H, 5.74. Found: C, 77.41; H, 5.53.

G2OH (6). Reduction of **5** (20.0 g, 26 mmol) by the general reduction procedure described above gave **6**. The crude solid was purified by dissolving in ethyl acetate and precipitating into hexanes to give a white solid, which was collected by filtration (17.9 g, 93%). Mp 101−105 °C. ^{1}H NMR ($CDCl_3$): δ 4.62 (s, 2H CH_2OH), 4.97 (s, 4H, Ar_1CH_2O), 5.03 (s, 8H, Ar_0CH_2O), 6.52 (t, 1H, Ar_2H), 6.56 (t, 2H, Ar_1H), 6.59 (d, 2H, Ar_2H) 6.67 (d, 4H Ar_1H), 7.24−7.47 (m, 20H, Ar_0H). SEC-LS: M_w 747 (nominal MW 745), $M_w/M_n = 1.00$.

G3CO$_2$CH$_3$ (8). Reaction of G2Br (**7)** (12.5 g, 15 mmol) and **1** (1.13 g, 6.7 mmol) by the general coupling procedure described above gave **8**. The product was purified by dissolving in methylene chloride and passing the solution through a short column of silica gel. Removal of the solvent under reduced pressure gave a light yellow oil that when dried further gave **8** as a colorless glass (10.08 g, 92%). ^{1}H NMR ($CDCl_3$): δ 3.87 (s, 3H, OCH_3), 4.95 (s, 8H, Ar_1CH_2O), 4.98 (s, 4H Ar_2CH_2O), 5.00 (s, 16H, Ar_0CH_2O), 6.55−6.78 (m, 19H, $Ar_{1-2}H$) 7.25−7.40 (m, 40H, Ar_0H, 2H, Ar_3H). SEC-LS: M_w 1642 (nominal MW 1622), $M_w/M_n = 1.00$. Anal. Calcd for ($C_{104}H_{92}O_{16}$): C, 78.50; H, 5.72. Found: C, 78.55; H, 5.45.

G3OH (9). Reduction of **8** (8.00 g, 4.9 mmol) by the general reduction procedure described above gave **9**. The crude product was purified by flash chromatography using silica gel, eluting with 80:20 (v:v) ethyl acetate/hexanes. A colorless glass was collected upon removal of the solvent under reduced pressure (7.59 g, 97%). ^{1}H NMR ($CDCl_3$): δ 4.58 (d, 2H, CH_2OH), 4.95 (s, 12H, $Ar_{1-2}CH_2O$), 5.01 (s, 16H, Ar_0CH_2O), 6.52 (m, 3H, Ar_3H), 6.56 (t, 4H, Ar_2H), 6.57 (t, 2H, Ar_2H), 6.64 (d, 4H, Ar_1H), 6.66 (d, 8H, Ar_1H), 7.25−7.40 (m, 40H, Ar_0H). SEC-LS: M_w 1582 (nominal MW 1594), $M_w/M_n = 1.00$.

G4CO$_2$CH$_3$ (11). Reaction of G3Br (**10)** (3.00 g, 1.8 mmol) and **1** (0.145 g, 0.86 mmol) by the general coupling procedure described above gave **11**. The crude product was purified by dissolution in methylene chloride and passing the solution through a short column of silica gel. Purification yielded a colorless glass upon removal of the solvent under reduced pressure (2.60 g, 91%). ^{1}H NMR ($CDCl_3$): δ 3.82 (s, 3H, OCH_3), 4.93 (s, 12H, $Ar_{2-3}CH_2O$), 4.95 (s, 16H, Ar_1CH_2O), 5.00 (s, 32H, Ar_0CH_2O), 6.53−6.66 (m, 43H, $Ar_{1-4}H$), 7.16−7.40 (m, 80H, Ar_0H, 2H, Ar_4H). SEC-LS: M_w 3270 (nominal MW 3321), $M_w/M_n = 1.01$. Anal. Calcd for ($C_{218}H_{188}O_{32}$): C, 78.87; H, 5.71. Found: C, 78.57; H, 5.84.

G4OH (12). Reduction of **11** (2.5 g, 0.752 mmol) by the general reduction procedure described above gave **12**. The crude oil collected was purified by flash chromatography using 25:1 (v:v) methylene chloride/diethyl ether as the solvent. The product was collected as a colorless glass after removal of the solvent under reduced pressure (2.18 g, 88%). ^{1}H NMR ($CDCl_3$): δ 4.50 (d, 2H, CH_2OH), 4.90 (s, 28H, $Ar_{1-3}CH_2O$), 4.96 (s, 32H, Ar_0CH_2O), 6.50−6.64 (m, 45H, $Ar_{1-4}H$), 7.26−7.38 (m, 80H, Ar_0H). SEC-LS: M_w 3277 (nominal MW 3293), $M_w/M_n = 1.01$.

G4OMs (13). Reaction of **12** (1.00 g, 0.304 mmol) in anhydrous THF with 5 equiv each of triethylamine and mesyl chloride with gentle stirring at room temperature under nitrogen for 12 h gave **13**. Once complete, ca. 100 mL of water was added and the solution extracted three times with methylene chloride. The collected organic layers were then washed with water and dried over anhydrous sodium sulfate and filtered, and the solvent was removed under reduced pressure. The crude product was purified by flash chromatography with 2% THF in methylene chloride as the solvent. The product was dried under vacuum to give **13** as a colorless glass (0.99 g, 97%). ^{1}H NMR ($CDCl_3$): δ 2.72 (s, 3H, SO_2CH_3), 4.87−4.97 (m, 60H, $Ar_{0-3}CH_2O$), 6.48−6.63 (m, 45H, $Ar_{1-4}H$), 7.24−7.36 (m, 80H, Ar_0H).

1-Hydroxypyrene (14).[13] Pyrene carboxaldehyde (7.00 g, 30 mmol) and *m*-chloroperbenzoic acid (11.26 g, 45.6 mmol) were dissolved in dry methylene chloride and refluxed with stirring under argon for 24 h. The solution was concentrated under reduced pressure to give a red-brown residue. To this residue 75 mL of a 10% $NaHCO_3$ solution was added with stirring, resulting in effervescence. Once the effervescence ceased, the remaining methylene chloride was removed under reduced pressure to give a dark purple solution and a precipitate. The precipitate was collected by filtration, washed with water, and allowed to dry, giving a brown solid. This solid was dissolved in a 1:1 (v:v) mixture of methanol (30 mL) and THF (30 mL), then 10.0 mL of 25% aqueous KOH solution was added to this mixture, which was then stirred under argon for 4 h. The mixture was concentrated under reduced pressure, diluted with 150 mL of a 2% aqueous KOH solution, and extracted two times with a 1:1 (v:v) benzene/diethyl ether mixture (200 mL each) to remove unreacted aldehyde and other organic impurities. The aqueous layer was collected and cooled in an ice bath and then acidified to a pH of 2 with concentrated HCl, resulting in the formation of a precipitate. The precipitate was collected by filtration and washed with water and then with 10% $NaHCO_3$. This yielded a black solid, which was dried under vacuum. The product was purified by flash chromatography using 75:25 (v:v) hexanes/ethyl acetate. The product elutes as a yellow band that glows yellow-green under long wavelength UV light. Removal of the solvent under reduced pressure gives a yellow solid (1.96 g, 30%). Mp 172−174 °C (lit. 178−180 °C). ^{1}H NMR ($CDCl_3$): δ 7.62−7.64 (d, 1H, Ar′H), 7.90−8.16 (m, 7H, Ar′*H*), 8.42−8.45 (d, 1H, Ar′*H*), 9.47 (s, 1H, O*H*). Anal. Calcd for ($C_{16}H_{10}O$): C, 88.05; H, 4.62. Found: C, 87.59; H, 4.47.

1-Methoxypyrene (15).[14] A solution of 1-hydroxypyrene **14** (0.200 g, 0.916 mmol), methyl iodide (0.57 mL 9.2 mmol), and potassium carbonate (0.252 g, 1.8 mmol) in dry THF was refluxed under argon with stirring for 3−4 days until no 1-hydroxypyrene was present by TLC (3:1 v:v hexanes/ethyl acetate). Once complete, the reaction was cooled and the solvent removed under reduced pressure. The residue was dissolved in water and methylene chloride and was extracted three times with methylene chloride. The combined organic layers were then washed with water and dried over anhydrous sodium sulfate. The solution was filtered and the solvent removed under reduced pressure to yield a yellow oil. The crude product was purified by column chromatography using 3:1 (v:v) hexanes/ethyl acetate as the solvent: the first band contained the product and the second band unreacted **14**. The chromatography was easily followed with long wavelength UV. Removal of the solvent gave **15** as a yellow oil that solidified upon standing (0.180 g, 85%). Mp 74−77 °C. λ_{max} (CH_2Cl_2) 352 nm, log ϵ 4.25. ^{1}H NMR ($CDCl_3$): δ 4.20 (s, 3H, OCH_3), 7.71−7.74 (d, 1H, Ar′*H*), 7.96−8.24 (m, 7H, Ar′*H*), 8.42−8.45 (d, 1H, Ar′*H*). Anal. Calcd for ($C_{17}H_{12}O$): C, 87.90; H, 5.21. Found: C, 87.47; H, 5.06.

General Procedure for Coupling of (G-*n*) Benzyl Bromide with 1-Hydroxypyrene (14).[15] To a solution of **14**

(1 equiv) and G-*n* benzyl bromide (1.5 equiv) in either dry acetone or THF was added 2.5 equiv of potassium carbonate and 0.2 equiv of 18-crown-6 (for generation 2 and higher). The reactions were followed by thin-layer chromatography while refluxing with stirring under argon. Once **14** had completely reacted, the reaction was cooled and 1−5 equiv of sodium hydroxide was added to convert the excess G-*n* benzyl bromide to G-*n* benzyl alcohol. The solvent was removed under reduced pressure and the residue dissolved in a mixture of water and methylene chloride. The solution was then extracted three times with methylene chloride. The collected organic layers were washed with 10% NaOH and then with water and finally dried over anhydrous sodium sulfate. The solution was then filtered and the solvent removed under reduced pressure. The crude products were then purified by the procedures described below.

G0Py (16). Reaction of **14** (0.300 g, 1.4 mmol) with benzyl bromide (0.244 mL, 2.0 mmol) in acetone following the general procedure described above gave **16**. The product was purified by flash chromatography using 9:1 (v:v) toluene/petroleum ether to give a light brown solid. This solid was dissolved in 3:1 (v:v) hexanes/ethyl acetate and passed through a short column of Florisil. The solvent was removed under reduced pressure to give **16** as a red oil that solidified to a light brown solid upon standing (0.37 g, 88%). Mp 101−105 °C. λ_{max} (CH_2Cl_2) 352 nm, log ϵ 4.17. ^{1}H NMR ($CDCl_3$): δ 5.55 (s, 2H, Ar_0CH_2O), 7.38−7.49 (m, 5H, Ar_0H), 7.67−7.69 (d, 1H, Ar′*H*), 7.82−8.24 (m, 7H, Ar′*H*), 8.50−8.53 (d, 1H, Ar′*H*). ^{13}C NMR ($CDCl_3$): 71.4 (Ar_0CH_2O), 110.1 (Ar′ C2), 121.1 (Ar′), 121.8 (Ar′), 124.7 (Ar′), 124.8 (Ar′), 125.6 (Ar′), 125.9 (Ar′), 126.0 (Ar′), 126.4 (Ar′), 126.8 (Ar′), 127.0 (Ar′), 127.7 (Ar′), 127.9 (Ar_0), 128.5 (Ar_0), 129.1 (Ar_0), 132.1 (Ar′), 132.2 (Ar′), 137.6 (Ar_0), 153.2 (Ar′ C1). Anal. Calcd for ($C_{23}H_{16}O$): C, 89.58; H, 5.23. Found: C, 88.83; H, 5.09.

G1Py (17). Reaction of **4** (0.684 g, 1.8 mmol) with **14** (0.300 g, 1.4 mmol) in anhydrous tetrahydrofuran following the general coupling procedure gave **17**. The product was purified by precipitation into hexane from methylene chloride, yielding a light brown solid. The solid was then dissolved in ethyl acetate and passed through a short column of Florisil followed by washing with excess solvent. Removal of the solvent under reduced pressure gave **17** as a red-brown oil that became solid upon standing (0.558 g, 78%). Mp 111−113 °C. λ_{max} (CH_2Cl_2) 352 nm, log ϵ 4.18. ^{1}H NMR ($CDCl_3$): δ 5.16 (s, 4H, Ar_0CH_2O), 5.49 (s, 2H, Ar_1CH_2O), 6.70 (s, 1H, Ar_1H), 6.95 (s, 2H, Ar_1H), 7.31−7.49 (m, 10H, Ar_0H), 7.78−7.81 (d, 1H, Ar′*H*), 7.95−8.22 (m, 7H, Ar′*H*), 8.48−8.51 (d, 1H, Ar′*H*). ^{13}C NMR ($CDCl_3$): 70.63 (Ar_0CH_2O), 71.22 (Ar_1CH_2O), 102.1 (Ar_1), 106.7 (Ar_1), 110.1 (Ar′ C2) 121.1 (Ar′), 121.8 (Ar′), 124.7 (Ar′), 124.8 (Ar′), 125.6 (Ar′), 125.9 (Ar′), 126.0 (Ar′), 126.6 (Ar′), 127.0 (Ar′), 127.9 (Ar′), 128.0 (Ar_0), 128.5 (Ar_0), 129.1 (Ar_0), 131.5 (Ar′), 132.2 (Ar′), 137.2 (Ar_0), 140.1 (Ar_1), 153.1 (Ar′ C1), 160.7 (Ar_1). SEC-LS: M_w 543 (nominal MW 521), M_w/M_n = 1.02. Anal. Calcd for ($C_{37}H_{28}O_3$): C, 85.36; H, 5.42. Found: C, 84.87; H, 5.18.

G2Py (18). Reaction of **7** (1.06 g, 1.3 mmol) and **14** (0.300 g, 1.4 mmol) by the general procedure in anhydrous tetrahydrofuran gave **18**. The product was purified by recrystallization in acetonitrile giving a white solid. The solid was then dissolved in 3:2 (v:v) ethyl acetate/hexanes and passed through a short column of Florisil followed by washing with excess solvent. Removal of the solvent under reduced pressure gave **18** as an oil that solidified to a cream-colored solid upon standing (1.105 g, 85%). Mp 123−127 °C. λ_{max} (CH_2Cl_2) 352 nm, log ϵ 4.37. ^{1}H NMR ($CDCl_3$): δ 5.09 (s, 8H, Ar_0CH_2O), 5.11 (s, 4H, Ar_1CH_2O), 5.47 (s, 2H, Ar_2CH_2O), 6.62−6.94 (m, 9H, $Ar_{1-2}H$), 7.27−7.45 (m, 20H, Ar_0H), 7.77−7.80 (d, 1H, Ar′*H*), 7.97−8.21 (m, 7H, Ar′*H*), 8.47−8.50 (d, 1H, Ar′*H*). ^{13}C NMR ($CDCl_3$): 70.5 ($ArCH_2O$), 70.6 ($ArCH_2O$), 71.2 (Ar_2CH_2O), 102.1 (Ar_{1-2}), 106.9 (Ar_{1-2}), 110.2 (Ar′ C2), 121.1 (Ar′), 121.8 (Ar′), 124.8 (Ar′), 125.7 (Ar′), 125.9 (Ar′), 126.0 (Ar′), 126.6 (Ar′), 127.1 (Ar′), 127.7 (Ar′), 128.1 (Ar_0), 128.5 (Ar_0), 129.1 (Ar_0), 132.1 (Ar′), 132.2 (Ar′), 137.3 (Ar_0), 139.8 (Ar_1), 140.2 (Ar_2), 153.1 (Ar′ C1), 160.6 (Ar_2), 160.7 (Ar_1). SEC-LS: M_w 932 (nominal MW 945), M_w/M_n = 1.02. Anal. Calcd for ($C_{65}H_{53}O_7$): C, 82.51; H, 5.65. Found: C, 82.72; H, 5.54.

G3Py (19). Reaction of **14** (0.076 g, 0.347 mmol) with **10** (0.69 g, 0.416 mmol) using the general coupling procedure in dry THF gave **19**. The crude product was purified by flash chromatography using methylene chloride as the solvent. The product was collected as a yellow band that gave **19** as a light yellow glass when the solvent was removed under reduced pressure (0.580 g, 93%). λ_{max} (CH_2Cl_2) 348 nm, log ϵ 4.40. ^{1}H NMR ($CDCl_3$): δ 5.01 (s, 8H, Ar_1CH_2O), 5.04 (s, 16H, Ar_0CH_2O), 5.07 (s, 4H, Ar_2CH_2O), 5.39 (s, 2H, Ar_3CH_2O), 6.59−6.90 (m, 21H, $Ar_{1-3}H$), 7.26−7.43 (m, 40H, Ar_0H), 7.69−7.72 (d, 1H, Ar′*H*), 7.90−8.16 (m, 7H, Ar′*H*), 8.42−8.46 (d, 1H, Ar′*H*). ^{13}C NMR ($CDCl_3$): 70.6 ($Ar_{0-2}CH_2O$), 71.2 (Ar_3CH_2O), 102.1, (Ar_{1-3}), 106.8 (Ar_{1-3}), 110.2 (Ar′ C2), 121.1 (Ar′), 121.7 (Ar′), 124.8 (Ar′), 125.6 (Ar′), 125.9 (Ar′), 126.6 (Ar′), 127.1 (Ar′), 127.7 (Ar′), 128.0 (Ar_0), 128.4 (Ar_0), 129.0 (Ar_0), 132.1 (Ar′), 137.2 (Ar_0), 139.7 (Ar_1), 139.8 (Ar_2), 140.1 (Ar_3), 153.1 (Ar′ C1), 160.5 (Ar_3), 160.6 (Ar_{1-2}). SEC-LS: M_w 1822 (nominal MW 1795), M_w/M_n = 1.01. Anal. Calcd for ($C_{121}H_{100}O_{15}$): C, 81.00; H, 5.62. Found: C, 80.81; H, 5.45.

G4Py (20). Reaction of **13** (0.100 g, 0.0297 mmol) with **14** (0.0071 g, 0.0326 mmol) using the general procedure in dry THF gave **20**. The crude product was purified by flash chromatography using 1% 2-propanol in methylene chloride as the eluent. The product was collected, and the solvent was removed under reduced pressure to yield **20** as a colorless glass (0.080 g, 77%). λ_{max} (CH_2Cl_2) 352 nm, log ϵ 4.46. ^{1}H NMR ($CDCl_3$): δ 4.85−4.95 (m, 60H, $Ar_{0-3}CH_2O$), 5.30 (s, 2H, Ar_4CH_2O), 6.50−6.62 (m, 45H, $Ar_{1-4}H$), 7.24−7.34 (m, 80H, Ar_0H), 7.42−7.46 (d, 1H, Ar′*H*), 7.80−8.05 (m, 7H, Ar′*H*), 8.40−8.45 (d, 1H, Ar′*H*). ^{13}C NMR ($CDCl_3$): 70.5 ($Ar_{0-3}CH_2O$), 71.2 (Ar_4CH_2O), 102.1 (Ar_{1-4}), 106.9 (Ar_{1-4}), 110.2 (Ar′ C2), 121.1 (Ar′), 121.7 (Ar′), 124.7 (Ar′), 125.7 (Ar′), 125.9 (Ar′), 126.0 (Ar′), 126.6 (Ar′), 127.1 (Ar′), 127.7 (Ar′), 128.0 (Ar_0), 128.5 (Ar_0), 129.0 (Ar_0), 132.1 (Ar′), 137.2 (Ar_0), 139.7 (Ar_1), 139.8 (Ar_{2-3}) 140.1 (Ar_4), 153.1 (Ar′ C1), 160.5 (Ar_4), 160.6 (Ar_{1-3}). SEC-LS: M_w 3495 (nominal MW 3492), M_w/M_n = 1.01. Anal. Calcd for ($C_{233}H_{196}O_{31}$): C, 80.14; H, 5.66. Found: C, 79.51; H, 5.59.

Results

I. Synthesis and Characterization. The poly(aryl ether) monodendrons were prepared by a variation of the synthetic route developed by Frechet,[10a] shown in Scheme 1. As with most convergent dendrimer syntheses,[1] an activated and protected A_2B monomer is required. This monomer, methyl 3,5-dihydroxybenzoate (**1**), was prepared by Fischer esterification of 3,5-dihydroxybenzoic acid with methanol.[10] Monodendron synthesis began with coupling of **1** with 2 equiv of benzyl bromide in the presence of potassium carbonate to give an ester-focused first generation monodendron, methyl 3,5-dibenzyloxybenzoate (**2,** $G1CO_2CH_3$).[10a,11] The ester functionality was then reduced[10b,12] with lithium borohydride (prepared in situ) to give benzyl alcohol (**3**, G1OH) which was then brominated[10a] to give the first generation benzyl bromide (**4**, G1Br). Two equivalents of this compound were then coupled with monomer **1** to give second generation ester **5** ($G2CO_2CH_3$), and the sequence continued as shown in Scheme 1. Bromination of **12** was only sporadically successful; this compound was more consistently activated by preparation of the mesylate, **13**.

The pyrene-focused monodendrons were synthesized by coupling of **14** with the corresponding benzyl bromide focused monodendrons in the presence of potassium carbonate as shown in Scheme 2. **14** was prepared by a literature synthesis.[13] The fourth generation compound **20** was prepared from mesylate **13** rather than the bromide. All isolated yields from the 1-hydroxypyrene coupling reactions were above 75%. The pyrene-focused

Scheme 1. Synthesis of Monodendrons

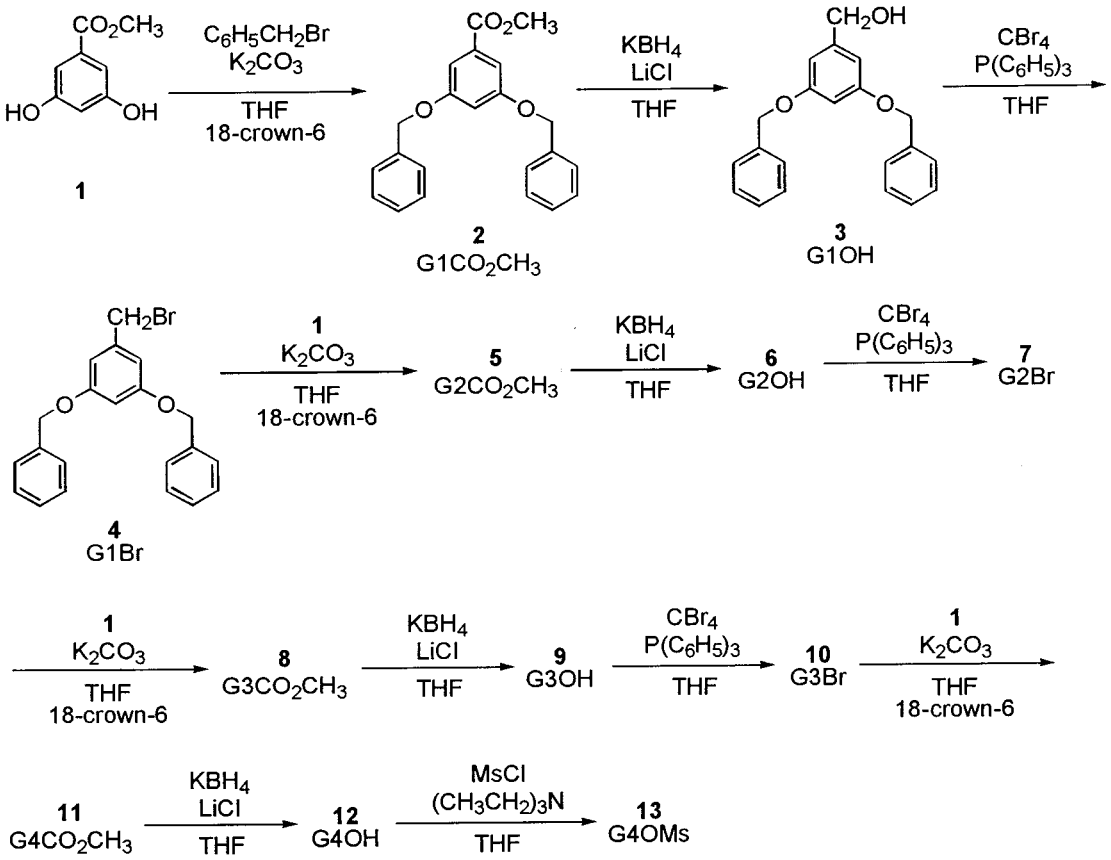

Scheme 2. Synthesis of Pyrene-Focused Monodendrons

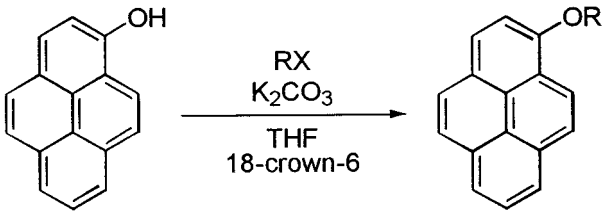

15 MeOPy, R = CH_3 , X = I
16 G0OPy, R = $C_6H_5CH_2$, X = Br
17 G1OPy, R = G1 , X = Br
18 G2OPy, R = G2 , X = Br
19 G3OPy, R = G3 , X = Br
20 G4OPy, R = G4 , X = OMs

monodendrons synthesized and studied in this report are shown in Figure 1.

The monodendrons were characterized by ^1H and ^{13}C NMR, size exclusion chromatography with light scattering detection (SEC-LS), and elemental analysis. The benzyl alcohol- and benzyl bromide-focused monodendrons are known compounds[10a] and gave comparable NMR data to the literature reports. The ester-focused monodendrons and pyrene-focused monodendrons are new compounds and were more fully characterized. The NMR spectrum of **18** is shown in Figure 2. SEC-LS has been shown to be an excellent method for determination of molecular weights for dendritic polymers.[12b,16] All monodendrons gave good SEC-LS data, and the results for the pyrene-focused monodendrons are listed in Table 1. Figure 3 shows SEC traces for the pyrene-focused monodendrons **17**−**20**.

The pyrene-focused monodendrons are electrochemically active as a result of the pyrene moiety.[17] Cyclic voltammetry (CV) of the monodendrons revealed a reversible oxidation of the pyrene moiety localized at approximately 1.3 V vs the normal hydrogen electrode and a second irreversible oxidation at approximately 2.0 V vs the normal hydrogen electrode. The first oxidation is completely reversible if the scan is reversed before the second oxidation. This second oxidation is irreversible and resulted in the deposition of a passivating film on the electrode surface. The cyclic voltammograms of G3Py **19** and G4Py **20** showed some distortion which may be a result of slow diffusion. Reversible and irreversible voltammograms are provided in the Supporting Information.

The pyrene-focused monodendrons are 1-alkoxypyrenes and show some spectral differences from pyrene.[18] The electronic absorption spectra and emission spectra of 1-alkoxypyrenes show fewer vibronic bands and are shifted slightly to longer wavelength. The solvent effect on the intensity of the vibronic bands which is observed for pyrene (known as the Ham effect)[19] is not observed for 1-alkoxypyrenes. There is a weak dependence of λ_{max} on solvent polarity for both absorption and emission. The absorption λ_{max} shifts from 352 nm in cyclohexane to 346 nm in acetonitrile. The emission λ_{max} shifts from 383 nm in cyclohexane to 381 nm in acetonitrile. Absorption and emission spectra of 1-methoxypyrene **15** in THF are shown in Figure 4.

II. Spectroscopic Studies. Pyrene was employed as the fluorophore to take advantage of its intense fluorescence and well-studied photochemistry.[20] The photophysics of 1-alkoxypyrenes are not identical with pyrene: along with the minor spectral changes described above, the fluorescence lifetimes of 1-alkoxy-

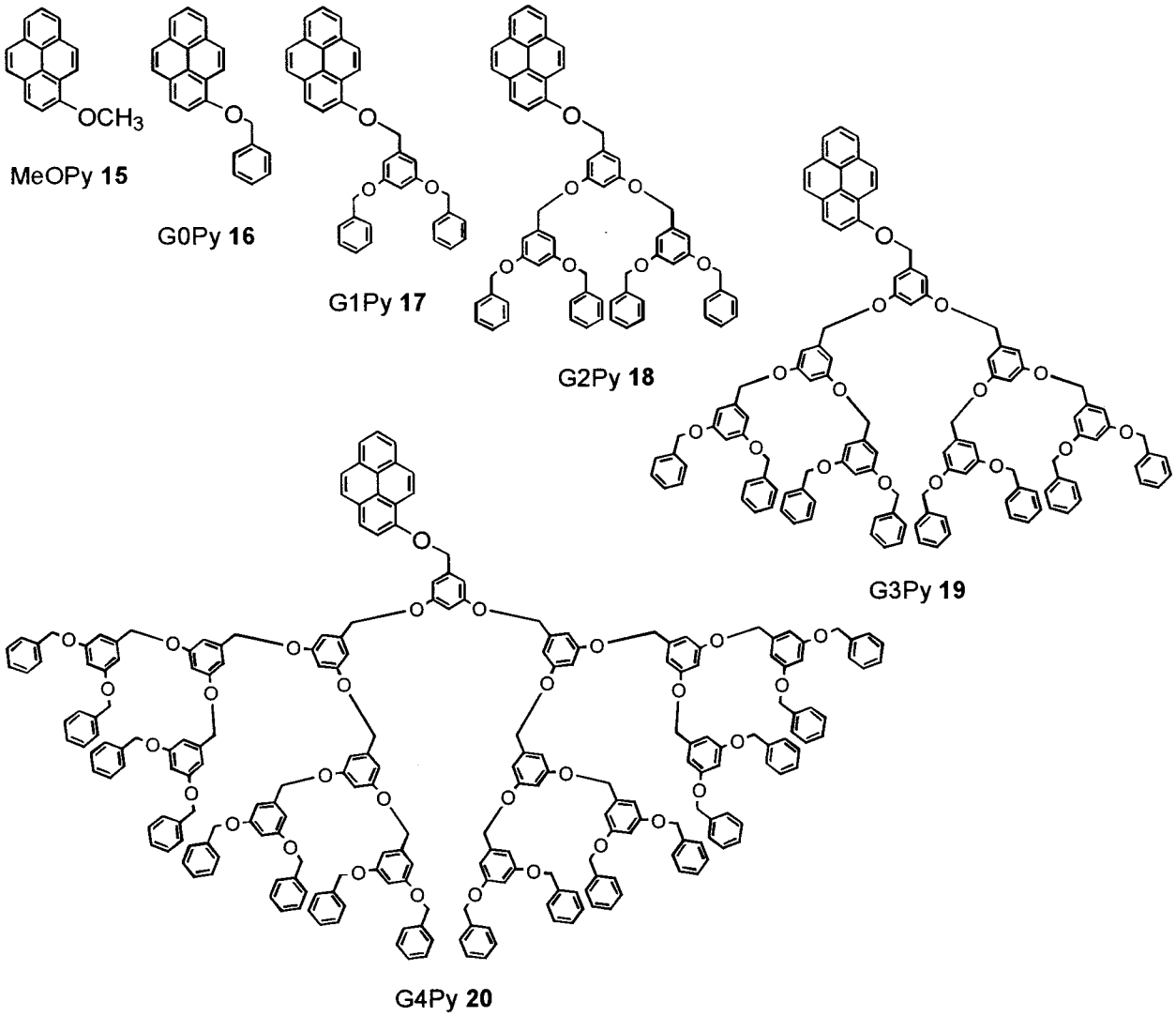

Figure 1. Structures of pyrene-focused monodendrons.

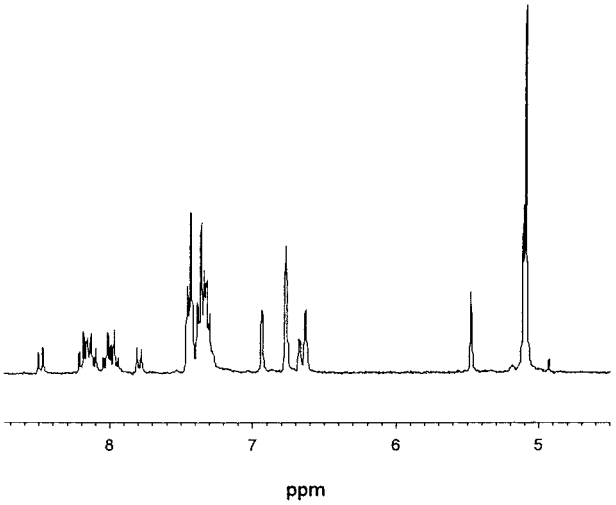

Figure 2. 300-MHz NMR spectrum of G2Py **18** in acetone-d_6. Peak assignments can be found in the Experimental Section.

pyrenes are significantly shortened and only weakly dependent on solvent.

Fluorescence lifetimes of the pyrene-focused monodendrons were measured using the phase modulation technique.[9] Lifetimes in anaerobic solvents (τ_o) are listed in Table 2. In tetrahydrofuran (THF), τ_o was found to be 20.7 ± 0.2 ns for all 1-alkoxypyrenes. In acetonitrile, τ_o was found to be 23.6 ± 0.2 ns for all 1-alkoxypyrenes except **15**, which had a somewhat shorter lifetime of 22.1 ns. In cyclohexane, τ_o was found to be 23.7 ± 0.9 ns for all 1-alkoxypyrenes, although G4Py **20** was insoluble in cyclohexane. We have also measured the lifetimes of these compounds by pulsed laser excitation, and similar results were obtained.[18]

Table 1. SEC Data for Pyrene-Focused Monodendrons

compound	nominal MW	M_w[a]	M_w/M_n[b]	$\delta n/\delta c$[c]
G1Py **17**	521	543	1.02	0.275
G2Py **18**	945	932	1.02	0.246
G3Py **19**	1795	1822	1.01	0.222
G4Py **20**	3492	3495	1.01	0.183

[a] M_w calculated from 90° light scattering and refractive index data using software from Precision Detectors. [b] M_w/M_n calculated from 90° light scattering and refractive index data using software from Precision Detectors. [c] $\delta n/\delta c$ in THF calculated from sample mass and refractive index data using software from Precision Detectors.

Pyrene is efficiently quenched by molecular oxygen, and oxygen quenching is well established in the photochemistry of pyrene and related aromatic hydrocarbons.[20,21] The quenching mechanism is collisional and is typically diffusion controlled.[22] Accordingly, oxygen

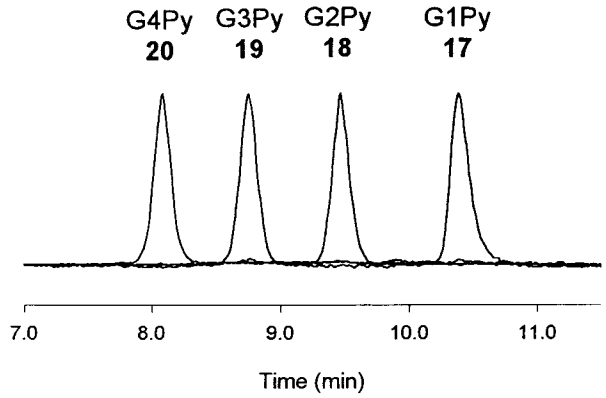

Figure 3. Size exclusion chromatograms of pyrene-focused monodendrons **17**−**20** in THF.

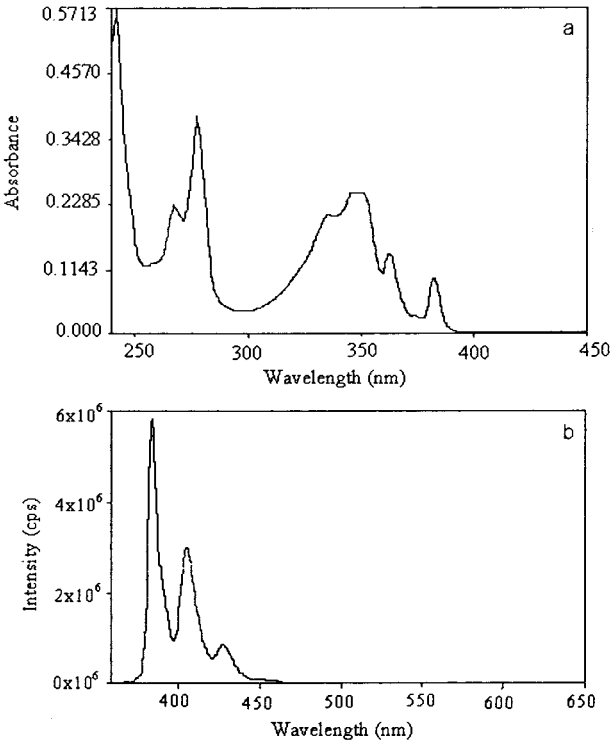

Figure 4. (a) Absorbance spectrum of 1-methoxypyrene **15** in THF at 1.0×10^{-5} M. (b) Emission spectrum of 1-methoxypyrene **15** in THF at 1.0×10^{-7} M.

quenching has been often used for establishing the microenvironment of pyrene.[19,22,23] Oxygen quenching rates were measured by determining the fluorescence lifetime of solutions with two different oxygen concentrations. These concentrations were achieved by bubbling the solutions with air or with pure oxygen. The rate constant for quenching was established from the lifetime data by the Stern−Volmer method,[24] using eq 1

$$\tau_o/\tau = 1 + k_q\tau_o[O_2] \qquad (1)$$

Here τ_o is the native lifetime (anaerobic), τ is the lifetime in the presence of oxygen, k_q is the bimolecular quenching rate constant, and $[O_2]$ is the molar concentration of oxygen. The Stern−Volmer constant K_{SV} is equal to $k_q\tau_o$. The quenched lifetimes and quenching rate constants are listed in Table 2.

The development of pulsed-field-gradient NMR[8,25] provides a convenient and noninvasive method to selectively measure translational diffusion coefficients in solution. This technique has been used previously for dendritic polymers.[4] Diffusion coefficients were determined for the pyrene-focused monodendrons in THF-d_8, acetonitrile-d_3, and cyclohexane-d_{12} at 298 K using the method of Wu, Chen, and Johnson.[8] Diffusion coefficients of water and solvent were used as internal standards. The diffusion coefficients are listed in Table 3. Acetonitrile and cyclohexane are much poorer solvents for these monodendrons than THF, and not all of the compounds were sufficiently soluble for the NMR measurement. G4Py **20** could not be measured in acetonitrile, and only G0Py **16** could be measured in cyclohexane. The measured diffusion coefficients of pyrene and methoxypyrene **15** are consistent with known diffusion coefficients for pyrene, which has been measured as 1.48×10^{-5} cm^2 s^{-1} in *n*-heptane,[22] which has a viscosity of 3.87×10^{-4} Pa s: more viscous than acetonitrile, but less viscous than THF or cyclohexane.

Table 2. Photophysical Data for Pyrene-Focused Monodendrons

compound	τ_o (ns)[a]	τ (ns) air saturated[b]	τ (ns) O_2 saturated[c]	k_q (M^{-1} s^{-1})[d]
		tetrahydrofuran		
pyrene	346	16.8	3.8	3.67×10^{10}
15	20.1	10.2	3.4	3.35×10^{10}
G0Py **16**	20.9	10.2	3.3	3.40×10^{10}
G1Py **17**	20.5	10.8	3.8	2.95×10^{10}
G2Py **18**	20.8	11.2	3.9	2.79×10^{10}
G3Py **19**	20.7	11.3	4.1	2.68×10^{10}
G4Py **20**	20.7	12.4	4.5	2.27×10^{10}
		acetonitrile		
pyrene	328	12.3	2.8	4.00×10^{10}
15	22.1	8.3	2.4	4.02×10^{10}
G0Py **16**	23.2	8.2	2.4	4.14×10^{10}
G1Py **17**	23.6	8.9	2.9	3.50×10^{10}
G2Py **18**	23.6	9.3	3.0	3.31×10^{10}
G3Py **19**	23.5	9.8	3.3	3.00×10^{10}
G4Py **20**	23.9	10.2	3.6	2.76×10^{10}
		cyclohexane		
pyrene	415	14.6	3.5	2.60×10^{10} [e]
15	23.3	9.1	2.9	2.72×10^{10}
G0Py **16**	24.6	9.3	2.9	2.67×10^{10}
G1Py **17**	23.8	9.8	3.1	2.46×10^{10}
G2Py **18**	24.5	10.1	3.4	2.28×10^{10}
G3Py **19**	22.3	10.5	3.8	2.06×10^{10}

[a] Determined by the phase-modulation method in anaerobic solvent at 298 K. See Experimental Section for details. [b] Determined by the phase-modulation method in air-saturated solvent at 298 K. $[O_2]$ from ref 20b: 1.5 mM for THF, 1.9 mM in acetonitrile, 2.4 mM in cyclohexane. See Experimental Section for details. [c] Determined by the phase-modulation method in oxygen saturated solvent at 298 K. $[O_2]$ from ref 20b: 7.3 mM for THF, 9.1 mM in acetonitrile, 11.5 mM in cyclohexane. See Experimental Section for details. [d] Calculated from the τ data using eq 1, the $[O_2]$ as given above, and τ_o from experimental data above for pyrene in all solvents and methoxypyrene in acetonitrile. Average values used for τ_o for other alkoxypyrenes: 20.7 ns in THF, 23.6 ns in acetonitrile, 23.7 ns in cyclohexane. [e] The rate constant for quenching of pyrene by oxygen in cyclohexane has been reported as 2.5×10^{10} M^{-1} s^{-1} (ref 20b).

Discussion

I. Synthesis and Characterization. Preparation of the monodendrons by the alternative procedure described above was successful. Compared with the classic Frechet synthesis,[10a] this procedure employs an extra step for each generation, which increases the effort and decreases the overall yield slightly. Some advantages are the use of a milder reducing agent ($LiBH_4$ prepared

Table 3. Diffusion Coefficients, Radii, Volumes, and Densities from Pulsed-Field-Gradient NMR

compound	D_{py} ($cm^2\ s^{-1}$)[a]	R_{Stokes} (Å)[b]	V_{Stokes} ($Å^3$)[c]	ρ_{Stokes} (Da/$Å^3$)[d]	V_{free} ($Å^3$)[e]
		tetrahydrofuran			
pyrene	1.7×10^{-5} [f]	2.8	92	2.19	
15	1.7×10^{-5}	2.8	92	2.52	
G0Py **16**	1.3×10^{-5}	3.7	210	1.47	
G1Py **17**	0.97×10^{-5}	4.9	490	1.06	25
G2Py **18**	0.78×10^{-5}	6.1	950	0.99	106
G3Py **19**	0.48×10^{-5}	10	4200	0.43	2600
G4Py **20**	0.34×10^{-5}	14	11500	0.30	8400
		acetonitrile			
pyrene	2.3×10^{-5} [f]	2.6	74	2.72	
15	2.2×10^{-5}	2.7	82	2.82	
G0Py **16**	1.8×10^{-5}	3.3	150	2.06	
G1Py **17**	1.4×10^{-5}	4.1	289	1.80	
G2Py **18**	1.2×10^{-5}	4.9	490	1.92	
G3Py **19**	1.1×10^{-5}	5.4	660	2.72	
		cyclohexane			
pyrene	9.4×10^{-6} [f]	2.6	74	2.73	
G0Py **16**	8.7×10^{-6}	2.8	92	2.52	

[a] Calculated from NMR data as described in the Experimental Section. [b] Calculated from eq 2 using, $k_B = 1.381 \times 10^{-23}$ J/K, $T = 298$ K, and $\eta = 4.56 \times 10^{-4}$ Pa s for THF, $\eta = 3.69 \times 10^{-4}$ for acetonitrile, and $\eta = 8.94 \times 10^{-4}$ for cyclohexane (ref 36). [c] Calculated from R_{Stokes} given above, $V_{Stokes} = 4\pi/3(R_{Stokes})^3$. [d] Calculated from V_{Stokes} given above and MW, $\rho_{Stokes} = MW/V_{Stokes}$. [e] Calculated from V_{Stokes} given above and V_{vdw} from Table 3, $V_{free} = V_{Stokes} - V_{vdw}$. [f] The diffusion coefficient of pyrene has been reported as 1.48×10^{-5} in *n*-heptane (ref 22c), $\eta = 3.87 \times 10^{-4}$ Pa s (ref 36).

in situ rather than $LiAlH_4$) and increased synthetic flexibility, since the ester-focused monodendrons can be activated either by the reduction/bromination sequence to give polyethers or by alkaline hydrolysis to the acid to give polyesters. Some difficulties were encountered with the bromination step for higher generations, but activation as the mesylate gave good coupling results. Preparation of the pyrene-focused monodendrons by coupling with **14** proceeded in good yield. All compounds were readily purified by recrystallization or flash chromatography.

NMR spectroscopy of the monodendrons gave spectra consistent with the expected structures. The benzyl alcohol- and benzyl bromide-focused monodendrons have been reported in the literature,[10a] and the ester-focused monodendrons have a distinctive singlet from the methyl ester at 3.9 ppm, along with the expected resonances from the aromatic and methylene groups. The pyrene-focused monodendrons also gave the expected pyrene resonances as complex multiplets between 7.7 and 8.5 ppm (Figure 2).

SEC-LS is well established as an analytical technique for dendrimer synthesis.[10a,12b,16] Evaluation of the ester- and alcohol-focused monodendrons by SEC-LS gave molecular weights consistent with the structures and low polydispersities (<1.01), indicative of pure materials. The pyrene-focused monodendrons gave good molecular weight and polydispersity data (Table 1), confirming the structural characterization of these materials.

The electrochemistry of the pyrene-focused monodendrons gave the expected oxidation and reduction waves for the pyrene moiety.[17] There was some distortion of the CVs for the higher generations, which may be attributable to slow diffusion.

The pyrene-focused monodendrons are 1-alkoxypyrenes. This results in some observed spectral differences from pyrene itself, primarily shifts to longer wavelength and changes in vibronic structure.[18] This is not unexpected given the conjugation of the alkoxy group with the pyrene aromatic system and is observed for other alkoxyaromatics.[26] The 1-alkoxypyrenes are strongly fluorescent and are excellent subjects for photophysical and photochemical studies.

Table 4. Theoretical Values for Radii, Volumes, and Densities of the Pyrene-Focused Monodendrons

compound	R_{theory} (Å)[a]	V_{theory} ($Å^3$)[b]	ρ_{theory} (Da/$Å^3$)[c]	V_{vdw} ($Å^3$)[d]	R_{vdw} (Å)[e]	ρ_{vdw} (Da/$Å^3$)[f]
pyrene	(3.5)	180		181	3.5	1.12
15	(3.7)	210		205	3.7	1.13
G0Py **16**	7.2	1560	0.198	276	4.0	1.12
G1Py **17**	10.1	4320	0.120	465	4.8	1.12
G2Py **18**	13.0	9200	0.102	844	5.9	1.12
G3Py **19**	15.9	16800	0.107	1608	7.2	1.12
G4Py **20**	18.8	27800	0.126	3119	9.1	1.12

[a] Radii of fully extended structures calculated from models (ref 29). [b] Volume of fully extended structures, from radii given above, $V_{theory} = 4\pi/3(R_{theory})^3$. [c] Density of fully extended structures from V_{theory} above and MW, $\rho_{theory} = MW/V_{theory}$. [d] Van der Waals volumes calculated by the method of Bondi (ref 32). [e] Van der Waals radii derived from the V_{vdw} given above, $V_{vdw} = 4\pi/3(R_{vdw})^3$. [f] Density from V_{vdw} given above and MW, $\rho_{vdw} = MW/V_{vdw}$.

II. Diffusion Coefficients and Molecular Radii of the Monodendrons. The Stokes−Einstein equation (2) relates the diffusion coefficient D to the radius R of a diffusing particle.[22,27]

$$D = \frac{k_B T}{6\pi\eta R} \tag{2}$$

Here k_B is the Boltzmann constant, T the absolute temperature, and η the viscosity of the solvent. Viscosity can change by as much as 10% upon deuteration,[28] which will introduce some systematic error. The observed trends are not impacted by this error, however. The Stokes radii (R_{Stokes}) determined from the experimental diffusion coefficients are listed in Table 3; radii from molecular models for fully extended monodendrons[29] are listed in Table 4. The relatively low R_{Stokes} of 2.6−2.8 Å calculated for pyrene and 1-methoxypyrene in all solvents suggest that these molecules "slide" through the solvent edgewise, since the molecular dimensions of pyrene are $3 \times 8 \times 11$ Å.[23a] The value of 2.6−2.8 Å is in reasonable agreement with the 3 Å dimension. R_{Stokes} for the smaller monodendrons are also rather low. In THF, they increase by about 1.2 Å per generation from G0 through G2, then by about 4 Å from G2 through G4 (we shall refer to increases with generation as the "generational radial increment"). The latter value is greater than the increment of 2.9 Å predicted by molecular models for fully extended structures.[29] In acetonitrile, the generational radial increment from G0 through G2 is only 0.8 Å, and the increment from G2 to G3 decreases to 0.5 Å. G4 was insufficiently soluble in acetonitrile for diffusion measurement. The data in both solvents point to a structural difference between smaller monodendrons (G0 to G2) and larger ones (G3 and G4). In THF, a good solvent, the structures are expanded, but the smaller molecules are more free to rotate and may slide the aromatic rings through the solvent edgewise, while rotation in the larger molecules is restricted. The generational radial increment between G3 and G4 is slightly larger than that between G2 and G3, so there is even greater rotational hindrance in G4 than in G3. At the de Gennes dense packed limit,[2] even the outer layers of a fully extended dendrimer should

be restricted from rotation, and G4 must be closer to this limit than G3. The G4 monodendron has not reached this limit: some layers must still be able to either backfold or rotate to present a small profile to the solvent. In acetonitrile, a poor solvent, the smaller generational radial increments correspond to structures that are collapsed. The reduction in the generational radial increment from G2 to G3 in acetonitrile suggests that this collapse becomes more profound for larger structures. We were unable to determine the diffusion coefficient for G4Py **20**, but we are able to reach some conclusions from the fluorescence quenching data (vide infra).

The radii of linear polymers scale with the number of monomers N (proportional to molecular weight) by a power law relationship, $R = N^{\nu}$, with an exponential factor ν typically between 0.5 and 0.6.[30] Here R is a root-mean-squared radius derived from the end-to-end distance for a polymer chain in a self-avoiding random walk conformation, which at high molecular weights is proportional to the radius of gyration.[30] For fully extended, spherically symmetric dendrimers, the radius increases linearly with generation (each "layer" has the same thickness), while the number of monomers and molecular weight increase exponentially with generation. This results in a logarithmic relation between radius and N, $R = k \log N$. This radius is a core-to-terminus distance for fully extended dendritic branches. Our measurements are on monodendrons, which are not spherically symmetrical. Also, the measured radii are Stokes radii:[22,27] they represent the radius of an impermeable sphere that has the same "drag" as the irregularly shaped and somewhat permeable monodendrons rather than directly measuring an end-to-end or core-to-terminus distance. Given these caveats, it is still edifying to examine the relationship between the measured radii and molecular weight. A plot of R_{Stokes} vs MW is shown in Figure 5. In THF (Figure 5a), a power law with an exponent of 0.56 fits these data slightly better than a logarithmic relationship ($r^2 = 0.99$ vs 0.95); however, this may be an artifact from the change in generational radial increment at G2. In acetonitrile (Figure 5b), a logarithmic relationship is slightly better than a power law with an exponent of 0.28 ($r^2 = 0.98$ vs 0.96). We are currently working to increase the size of the data set to make these interpretations less speculative.

The Stokes−Einstein equation (2) has been modified for small and nonspherical molecules, since the underlying assumptions are questionable for such particles.[27,31] To correct for oblate or prolate ellipsoids, R in eq 2 is replaced by $R(f/f_0)$, where R is now the radius of a sphere with the same volume as the diffusing particle and f/f_0 is the correction factor for the ellipsoid. Pyrene is an ellipsoid with an axial ratio of 3.1, which has a correction factor (f/f_0) of 1.1. The van der Waals volume (V_{vdw}) of pyrene calculated by the method of Bondi[32] is 181 Å^3, corresponding to a sphere with a radius of 3.5 Å. Using $(f/f_0) = 1.1$, eq 2 should give a radius of 3.9 Å. It is not unusual that the experimental radius from eq 2 is smaller (2.6−2.8 Å from our data). The numerical factor 6 in the denominator of eq 2 is strictly valid only for particles significantly larger than the solvent.[27,31] Hydrodynamic theories predict a lower limit of 4 for particles approximately the same size as the solvent, although other theoretical approaches and some experimental data suggest factors as small as 1.5.[27,31] Using a factor of 4 with our diffusion data gives Stokes radii of 3.9−4.2 Å for pyrene, in good agreement with the corrected value of 3.9 Å.

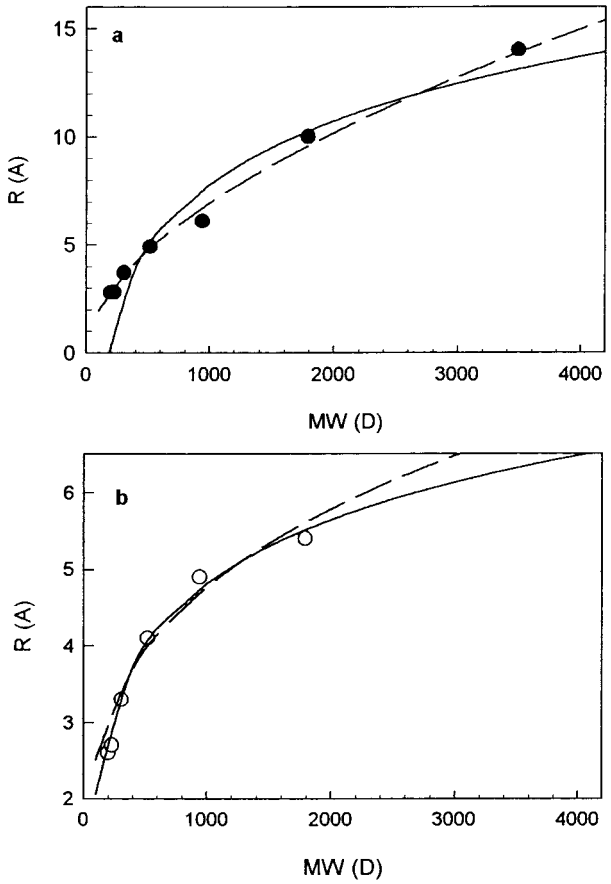

Figure 5. Plots of the Stokes radius (R_{Stokes}) as a function of molecular weight: (a) THF; (b) acetonitrile. Symbols are experimental data. The solid lines represent a logarithmic relationship between R_{Stokes} and MW. The dashed lines represent a power law relationship between R_{Stokes} and MW with an exponent of 0.56 for THF and 0.28 for acetonitrile.

Van der Waals volumes V_{vdw} and radii R_{vdw} can be calculated for the monodendrons,[32] and these are listed in Table 4. In THF, R_{vdw} is larger than R_{Stokes} for pyrene, methoxypyrene, and G0Py **16** (although corrections[27,31] can make agreement more reasonable), almost identical for G1Py **17** and G2Py **18**, and considerably smaller for G3Py **19** and G4Py **20**. The structures of the larger molecules in a good solvent like THF incorporate significant void space and solvent so R_{vdw} underestimates the true radius. The free volume can be calculated by taking the difference between V_{vdw} and a volume derived from the Stokes radius, V_{Stokes}. This free volume is listed in Table 3. In acetonitrile, V_{Stokes} is consistently smaller than V_{vdw}, so no free volume can be calculated. The agreement between R_{vdw} and R_{Stokes} for G1Py **17** and G2Py **18** in THF gives us confidence in using eq 2 to calculate R_{Stokes} for all molecules larger than G1. In acetonitrile, R_{vdw} is always larger than R_{Stokes}, showing the reduced extension in the poorer solvent. If microscopic details of solvent structure (rather than bulk properties such as viscosity) are significant in the mechanism of diffusion, the small size of acetonitrile compared to THF could also be responsible for the low R_{Stokes} in acetonitrile.

It is also useful to calculate molecular densities from the radii and molecular weights.[5a] These are listed in Table 4. Theoretical densities assuming fully extended

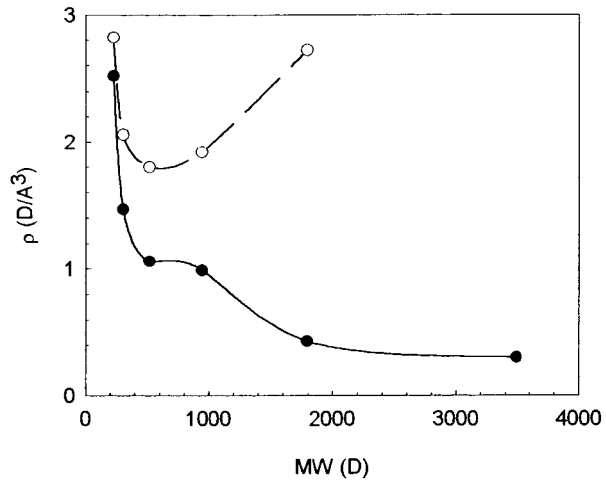

Figure 6. Plot of Stokes density (ρ_{Stokes}) as a function of molecular weight in THF (closed circles) and acetonitrile (open circles). Lines are interpolated from data points.

monodendrons decrease from G0 through G2, increase slightly for G3, and increase more dramatically for G4. This is expected, since molecular weight increases exponentially with generation while volume increases as the third power of generation. Eventually, the molecular weight increase exceeds the volume increase resulting in increased density. Experimental densities (ρ_{Stokes}) were calculated using V_{Stokes}. Different trends are found for ρ_{Stokes} in THF and acetonitrile. In THF, ρ_{Stokes} decreases from G0 to G4, with the largest decrease between G2 and G3, consistent with the change in generational radial increment between G2 and G3, and with expanded structures. In acetonitrile, ρ_{Stokes} decreases from G0 to G1, increases slightly for G2, and then increases dramatically for G3. This is consistent with the change in generational radial increment between G2 and G3 and with compressed structures. Densities in THF and acetonitrile as a function of molecular weight are shown in Figure 6.

It is interesting to compare the analyses in THF and acetonitrile. R_{Stokes} is always less than the theoretical radii for fully extended branches, and we assign this to rotational flexibility and backfolding. R_{Stokes} in THF is always larger than R_{Stokes} in acetonitrile. In both solvents there is a change in the generational radial increment between G2 and G3: in THF the generational radial increment increases, in acetonitrile the generational radial increment decreases. Between G2 and G3 the open structures of smaller dendrimers are replaced by the more spherical structures of larger dendrimers: spherical and extended in THF, spherical and compact in acetonitrile. The densities in acetonitrile are greater than those in THF. In THF, the density decreases from G0 to G4, with the largest difference between G2 and G3. In acetonitrile, the density reaches a minimum at G1 and increases sharply between G2 and G3.

Our data can also be compared to the data of Mourey,[6] Hult,[4] and DeSchryver.[5a] Mourey's viscometric study[6] on similar poly(aryl ether) monodendrons reported hydrodynamic radii in THF that are slightly larger than the Stokes radii reported here: 8 Å vs 6 Å for G2 poly(aryl ether) monodendrons, and 15 Å vs 14 Å for G4 monodendrons. Agreement is better for the larger monodendrons, where the Stokes−Einstein equation is more accurate, and the numbers are encouragingly similar, given the potential errors of the two methods. Above G2, Mourey reports a generational radial increment of 3.6 Å per generation, similar to our average increase of 4.0 Å per generation. The numerical data from Hult's NMR study of aliphatic polyester tridendrons[4] cannot be directly compared to our data, but it is significant that Hult observed a change in the generational radial increment at generation 3, similar to our observation at generation 2.

DeSchryver[7] used fluorescence depolarization to measure the hydrodynamic volumes of poly(aryl ether) didendrons with a rubicene core. These volumes derive from a Stokes relation similar to eq 2, but from rotational diffusion. Spherical objects can rotate without displacing solvent, while translational diffusion must displace solvent. There are some notable differences between their results and ours. In acetonitrile, a solvent common to both studies, their hydrodynamic volumes are significantly larger than those reported here. For molecules of similar molecular weight, their G1 didendron (MW = 962) has a volume of 3230 Å^3, while our G2Py monodendron **18** (MW = 945) has a volume of 490 Å^3. Their G2 didendron (MW = 1810) has a volume of 6590 Å^3, while our G3Py monodendron **19** (MW = 1795) has a volume an order of magnitude lower, 660 Å^3. Similar differences are found comparing volumes as a function of generation, multiplying the volumes for our monodendrons by a factor of 2 for comparison with their didendrons. If one compares their hydrodynamic volumes in toluene with those reported here in THF (both good solvents, although our experience suggests that THF is a better solvent), one finds that the volumes differ at low molecular weights but become similar at higher molecular weights. For the molecules with molecular weights near 950, their volume is 4030 Å^3 while ours is only 950 Å^3, but for molecules with molecular weights near 3500, their volume is 12 500 Å^3 while ours is 11 500 Å^3. Comparing volumes as a function of generation, a similar trend is observed: the volumes are quite different at low molecular weight but similar for higher molecular weight. An understanding of these discrepancies must await the results of further studies in progress. They could arise from several factors, including the different types of diffusion (rotational vs translational) and the different molecular architectures of monodendrons and didendrons.

II. Quenching Rates and Diffusion. The quenching rate constant k_q can be related to the sum of the diffusion coefficients of the reactants by a modified Smoluchowski equation (3).[33]

$$k_q = \alpha 4\pi(D_{Py} + D_{O_2})R_o N \qquad (3)$$

Here α is the quenching efficiency, R_o is the interaction radius for the quenching event, and N is Avogadro's number. For pyrene and dioxygen, α is believed to be unity[20−23] and R_o to be approximately 5.5 Å.[23a] The quantity $4\pi N$ is constant, and D_{O_2} should be constant for a given solvent and temperature; therefore, if α and R_o are constant for the monodendrons, then the experimentally determined k_q and D_{py} values should make a consistent data set. However, relatively large deviations are found, as much as 15−20% between methoxypyrene **15** and G4Py **20** in THF or G3Py **19** in acetonitrile. These deviations are too large to be the result of transient effects,[33] which arise from the time dependence of the true quenching rate constant. Furthermore, our deviations arise from comparisons between rate

Table 5. Analysis of Photophysical and Diffusion Data

compound	α_{exp}[a]	α_{calc}[b]	P_{rel}[c]	$D_{O_2} + D_{py}$ ($cm^2\ s^{-1}$)[d]	D_{O_2} ($cm^2\ s^{-1}$)[d]	η_{rel}[e]
				tetrahydrofuran		
pyrene		1.00		8.82×10^{-5}	7.12×10^{-5}	-
15		1.00		8.05×10^{-5}	6.35×10^{-5}	1.00
G0Py **16**		0.92		8.17×10^{-5}	6.87×10^{-5}	0.92
G1Py **17**	0.97	0.86	0.8	7.09×10^{-5}	6.12×10^{-5}	1.04
G2Py **18**	0.94	0.82	0.7	6.71×10^{-5}	5.93×10^{-5}	1.07
G3Py **19**	0.94	0.75	0.7	6.44×10^{-5}	5.96×10^{-5}	1.07
G4Py **20**	0.82	0.70	0.4	5.46×10^{-5}	5.12×10^{-5}	1.24
				acetonitrile		
pyrene		1.00		9.6×10^{-5}	7.3×10^{-5}	
15		1.00		9.7×10^{-5}	7.5×10^{-5}	1.00
G0Py **16**		0.93		9.9×10^{-5}	8.1×10^{-5}	0.91
G1Py **17**	0.96	0.88	0.7	8.4×10^{-5}	7.0×10^{-5}	1.06
G2Py **18**	0.92	0.84	0.5	8.0×10^{-5}	6.8×10^{-5}	1.09
G3Py **19**	0.85	0.83	0.1	7.2×10^{-5}	6.1×10^{-5}	1.21
G4Py **20**				6.6×10^{-5}	(5.6×10^{-5})[f]	(1.32) [f]
				cyclohexane		
pyrene				6.25×10^{-5}	5.31×10^{-5}	
15				6.54×10^{-5}		
G0Py **16**				6.42×10^{-5}	5.55×10^{-5}	
G1Py **17**				5.91×10^{-5}		
G2Py **18**				5.48×10^{-5}		
G3Py **19**				4.95×10^{-5}		

[a] Calculated from eq 3 using, $R_o = 5.5$ Å (ref 23a), $D_{O_2} = 6.35 \times 10^{-5}$ $cm^2\ s^{-1}$ in THF from methoxypyrene, $D_{O_2} = 7.4 \times 10^{-5}$ $cm^2\ s^{-1}$ in acetonitrile from pyrene and methoxypyrene. D_{O_2} has been determined to be 5.6×10^{-5} $cm^2\ s^{-1}$ in *n*-heptane ($\eta = 3.87 \times 10^{-4}$ Pa s) and 9.0×10^{-5} $cm^2\ s^{-1}$ in acetone ($\eta = 3.16 \times 10^{-4}$ Pa s) (ref 21a). [b] Calculated from eq 4 as described in the text. $R = 2.8$ Å for pyrene in THF, $R = 2.6$ Å for pyrene in acetonitrile, $R' = R_{Stokes} - R$. Values for R_{Stokes} for the monodendrons can be found in Table 2. [c] Calculated from eq 5 as described in the text. [d] Calculated from eq 3 using the experimental values for D_{py} and k_q, $R_o = 5.5$ Å. D_{O_2} has been determined to be 5.6×10^{-5} $cm^2\ s^{-1}$ in *n*-heptane ($\eta = 3.87 \times 10^{-4}$ Pa s) and 9.0×10^{-5} $cm^2\ s^{-1}$ in acetone ($\eta = 3.16 \times 10^{-4}$ Pa s) (ref 21a). [e] Calculated from eq 6 as described in the text. [f] Calculated assuming $D_{py} = 1.00 \times 10^{-5}$ cm^2/s for G4Py in acetonitrile.

constants determined by the Stern−Volmer method,[24] which does not correct for such transient effects. The experimentally determined rate constants will be time-averaged rate constants, and any errors from the neglect of transient effects should effectively cancel, since the errors will be of similar magnitude for all measurements.

There are several methods for treating the observed deviations in the quenching data. One simple explanation is that the monodendrons "shield" the fluorophore from the quencher, acting as a barrier to diffusing dioxygen.[34] This barrier will not be impermeable, but has reduced permeability (or increased viscosity). The data in THF and acetonitrile can be treated by varying the efficiency α in eq 3, using experimental values for D_{py} and the value for D_{O_2} determined from methoxypyrene, which is assumed to have no shielding. Experimentally determined values of α are listed in Table 5 as α_{exp}. The data can also be treated by determining D_{O_2} for each monodendron from experimentally determined k_q and D_{py} values and using these D_{O_2} values to establish relative viscosities. Experimentally determined D_{O_2} values are also listed in Table 5. Since we do not have D_{py} for most of the monodendrons in cyclohexane, our analysis of these data is limited. The sum of the diffusion coefficients from the Smoluchowski analysis ($D_{O_2} + D_{py}$) is given in Table 5, along with D_{O_2} for pyrene and G0Py **16**. As in THF and acetonitrile, the sum of the diffusion coefficients in cyclohexane for the larger monodendrons (G3 and G4) is smaller than

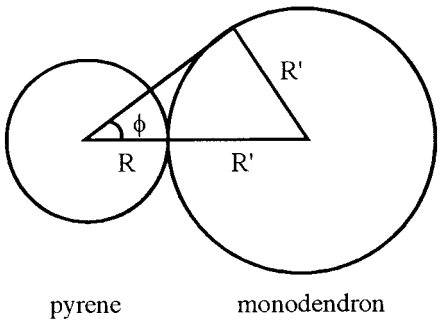

Figure 7. Shielding model based on two spheres touching at a single point. Circle C1 of radius R represents pyrene, and circle C2 with radius R' represents the monodendron. The angle $\phi = \sin^{-1}(R'/(R + R'))$. The fraction of the surface area of C1 occluded by C2 is $2\phi R/2\pi R$, or ϕ/π.

D_{O_2} from the pyrene or methoxypyrene analysis. This demonstrates that quenching of the pyrene fluorophore in these molecules cannot be diffusion controlled: there must be some shielding of the fluorophore.

A simple (and rather naive) model for shielding can be constructed by considering the pyrene-focused monodendrons as two spheres touching at a single point. The fraction F of the surface area of the first sphere (pyrene, radius R) shielded by the second (the monodendron, radius R') can be calculated from their radii, as shown in Figure 7.[35] For a first approximation, the monodendrons are assumed to be impermeable to dioxygen: the efficiency α_{calc} then equals the efficiency of pyrene (where $\alpha = 1$) minus the fraction shielded, as given in eq 4.

$$\alpha_{calc} = 1 - \frac{2R \sin^{-1}\left(\frac{R'}{R + R'}\right)}{2\pi R} \qquad (4)$$

The radius of pyrene R was assumed to be 2.8 Å in THF and 2.6 Å in acetonitrile (R_{Stokes} from the diffusion analysis), and the radii of the monodendrons R' were obtained by subtracting R from R_{Stokes} for the monodendrons. As described above, there are questions about R_{Stokes} for the smaller molecules, but we chose to use uncorrected radii rather than mix correction factors. The predicted efficiencies α_{calc} are given in Table 5. There are significant differences between the predicted (α_{calc}) and experimental (α_{exp}) quenching efficiencies for the smaller monodendrons in THF (G0 to G3) and acetonitrile (G0 to G2). This is consistent with open structures, allowing dioxygen to diffuse readily through the polymers. Such open structures have been predicted for smaller dendrimers.[2,3] The difference decreases for G4Py **20** in THF and G3Py **19** in acetonitrile, implying denser structures with reduced permeability. Note that the break in behavior for the quenching analysis is between G3 and G4 in THF but between G2 and G3 in acetonitrile. This solvent influence on shielding reflects the solvent influence on monodendron structure. This is consistent with the analysis of the diffusion data above for radii, volume, and density: acetonitrile is a poorer solvent giving more compact structures with greater shielding.

One can extend this model and determine relative permeabilities for the monodendrons. If the monodendrons were completely permeable (with permeability equal to the solvent), then no shielding would be observed and α_{exp} would be 1.00 for all monodendrons. If the monodendrons were impermeable (and the two-

sphere model completely valid), then α_{exp} would be equal to α_{calc}. By determining where α_{exp} falls between 1.00 and α_{calc}, one can determine a relative permeability, P_{rel}:

$$P_{rel} = \frac{\alpha_{exp} - \alpha_{calc}}{1 - \alpha_{calc}} \quad (5)$$

P_{rel} will scale from zero for impermeable polymers to unity for completely permeable polymers. The calculated P_{rel} for the pyrene-focused monodendrons in THF and acetonitrile are given in Table 5. The observed trends are as expected: decreasing permeability with increasing generation. The decrease is much greater in acetonitrile, consistent with a more compact structure. This model has obvious limitations: neither pyrene nor the monodendrons are spherical, the Stokes radii rest on certain assumptions, and the assumption that pyrene does not penetrate the monodendrons is unlikely to be realistic, particularly for the larger monodendrons.

A second approach is to determine dioxygen diffusion coefficients D_{O_2} from the Smoluchowski equation (3) and the experimental D_{py}. Since R for dioxygen remains constant, the D_{O_2} values can be used through the Stokes−Einstein relation (2) to calculate relative viscosities η_{rel} for the monodendron solutions.[27] If it is assumed that η is unperturbed for methoxypyrene, then η_{rel} can be calculated by

$$\eta_{rel} = \frac{\eta'}{\eta} = \frac{D_{O_2}}{D_{O_2}'} \quad (6)$$

Here η' is the apparent viscosity of the monodendron solution, η is the viscosity of the solvent, D_{O_2} is the diffusion coefficient for dioxygen from the methoxypyrene quenching and diffusion data, and D_{O_2}' is the diffusion coefficient for dioxygen from the monodendron quenching and diffusion data. η_{rel} values are given in Table 5. This approach assumes that the smaller values for D_{O_2} result from increased viscosity from the presence of the monodendrons. The strength of this approach is that it is less model dependent than the shielding approach, since certain errors will cancel. However, it should be recognized that in dilute solution, the oxygen molecules will mostly diffuse through bulk THF (with a relative viscosity of 1). The η_{rel} in Table 5 therefore will underestimate the true viscosity "within" the monodendrons. This approach also reveals a major change in structure between G3 and G4 in THF and between G2 and G3 in acetonitrile. There is also something unusual about G0, which appears to lower the viscosity of THF. We have observed that G0, or benzyloxypyrene, has slightly different behavior than all larger monodendrons. This may be an electronic effect from the 3,5-alkoxy substitution of the larger monodendrons. Alternatively, for the quenching analysis, oxygen may quench G0 by contact with the phenyl ring as well as by contact with the pyrene. This would require a different value of R_o in the Smoluchowski equation for accurate analysis. Given these observations, we have not used G0 as the reference compound for any of our analyses.

Our analysis of the cyclohexane data is limited by the lack of experimentally determined diffusion coefficients D_{py} in that solvent, except for pyrene and G0. We can calculate the sum of the diffusion coefficients ($D_{py} + D_{O_2}$) from the Smoluchowski analysis of the quenching data (Table 5), and the presence of shielding is confirmed by the values for G2Py **18** and G3Py **19**, which are near or below the value for D_{O_2} from the pyrene data. If a structural change occurs in cyclohexane, it is between G0 and G1 from the large change in ($D_{py} + D_{O_2}$). All monodendrons would then have a collapsed, compact structure in this very poor solvent.

Comparison with other photophysical studies[5] is not as productive as the comparison with other methods for determining radii. Many of the studies were on very different structures, and many quenching studies assumed nondiffusing polymers, assigning all changes in k_q to quencher diffusion. Frechet's early study of absorbance spectra of nitroaniline-focused monodendrons revealed a structural change between G3 and G4 in a variety of solvents,[5b] similar to our results in THF. Our study shows the difficulty in interpreting diffusion-controlled quenching data without firm knowledge of the diffusion coefficient of either fluorophore or quencher.

Conclusion

The experimentally determined diffusion coefficients for the pyrene-focused monodendrons are extremely powerful when combined with the photophysical data to give insight into the solution structure of dendritic materials. In THF, the calculated Stokes radii show that the poly(aryl ether) monodendrons are not fully extended ($R_{Stokes} < R_{theory}$) and that the smaller monodendrons (G0−G2) are more open and flexible than the larger ones (G3−G4). In acetonitrile, the structures are less extended (more collapsed), and there is a structural change between G2 and G3, with G3 even more compact. The quenching data reveal more: the smaller monodendrons (G0−G3 in THF, G0−G2 in acetonitrile) are a minimal barrier to the passage of a small molecule like dioxygen, while the larger monodendrons (G4 in THF, G3−G4 in acetonitrile) are more dense and less permeable. In cyclohexane, all monodendrons above G1 appear to have this denser structure. In THF, the change in behavior for the diffusion measurements is between G2 and G3 while for the quenching data it is between G3 and G4. This reflects the different sizes of the probe molecules: THF for the diffusion coefficients and dioxygen for the quenching studies. In acetonitrile, the change is between G2 and G3 for both types of measurements, a result of the more collapsed structures or the similar size of acetonitrile and dioxygen as probe molecules. The change in behavior in cyclohexane appears to be between G0 and G1 from the quenching data, consistent with the poorest solvent. Further studies in progress are expected to reveal more insights into the structure of dendritic polymers.

Acknowledgment. This research was supported by the National Science Foundation under Grant DMR-9412292. We thank Hye Jung Han for obtaining ^{13}C NMR spectra of the monodendrons.

Supporting Information Available: Synthetic details and characterization data for previously reported procedures and reversible and irreversible oxidative voltammograms of the pyrene-labeled poly(aryl ether) monodendrons. This material is available free of charge via the Internet at http://pubs.acs.org.

References and Notes

(1) (a) Tomalia, D. A.; Naylor, A. M.; Goddard, W. A., III *Angew. Chem., Int. Ed. Engl.* **1990**, *29*, 138. (b) Kim, Y. H. *Adv. Mater.* **1992**, *4*, 764. (c) Tomalia, D. A.; Durst, H. D. *Top.*

Curr. Chem. **1993**, *165*, 193. (d) Newkome, G. *Advances in Dendritic Macromolecules*; JAI Press: Greenwich, CT, 1994. (e) Frechet, J. M. J. *Science* **1994**, *263*, 1710. (f) Voit, B. I. *Acta Polym.* **1995**, *46*, 87. (f) Hawker, C. J.; Devonport, W. *Step-Growth Polymers for High Performance Materials;* Hedrick, J. L., Labadie, J. W., Eds.; ACS Symposium Series 624; American Chemical Society: Washington, DC, 1996, p 186.

(2) de Gennes, P. G.; Hervet, H. *J. Phys. Lett.* **1983**, *44*, L351.

(3) (a) Naylor, A. M.; Goddard, W. A., III; Kiefer, G. A.; Tomalia, D. A. *J. Am. Chem. Soc.* **1989**, *111*, 2339. (b) Lescanec, R. L.; Muthukumar, M. *Macromolecules* **1990**, *23*, 2280. (c) Mansfield, M. L.; Klushin, L. I. *Macromolecules* **1993**, *26*, 4262. (d) Murat, M.; Grest, G. S. *Macromolecules* **1996**, *29*, 1278. (e) Boris, D.; Rubinstein, M. *Macromolecules* **1996**, *29*, 7251. (f) Cai, C.; Chen, Z. Y. *Macromolecules* **1997**, *30*, 5104. (g) Miklis, P.; Cagin, T.; Goddard, W. A., III *J. Am. Chem. Soc.* **1997**, *119*, 7458.

(4) Ihre, H.; Hult, A.; Soderland, E. *J. Am. Chem. Soc.* **1996**, *118*, 6388.

(5) (a) De Backer, S.; Prinzie, Y.; Verheijen, W.; Smet, M.; Desmedt, K.; Dehaen, W.; DeSchryver, F. C. *J. Phys. Chem. A* **1998**, *102*, 5451. (b) Hawker, C. J.; Wooley, K. L.; Frechet, J. M. J. *J. Am. Chem. Soc.* **1993**, *115*, 4375. (c) Frank, R. S.; Merkle, G.; Gauthier, M. *Macromolecules* **1997**, *30*, 5397. (d) Pollak, K. W.; Leon, J. W.; Frechet, J. M. J.; Maskus, M.; Abruna, H. D. *Chem. Mater.* **1998**, *10*, 30. (e) Jiang, D.-L., Aida, T. *J. Am. Chem. Soc.* **1998**, *120*, 10895. (f) Sluch, M. I.; Scheblykin, I. G.; Varnavsky, O. P.; Vitukhnovsky, A. G.; Krasovskii, V. G.; Gorbatsevich, O. B.; Muzafarov, A. M. *J. Lumin.* **1998**, *76&77*, 246.

(6) Mourey, T. H.; Turner, S. R.; Rubinstein, M.; Frechet, J. M. J.; Hawker, C. J.; Wooley, K. L. *Macromolecules* **1992**, *25*, 2401.

(7) (a) Hanson, J. E.; Murphy, W. R., Jr.; Riley, J. M.; Tyler, T. L.; Kelley, S. O.; Makarewicz, A. M. *Polym. Mater. Sci. Eng.* **1995**, *73*, 358. (b) Hanson, J. E.; Khan, W. A.; Murphy, W. R., Jr. *Polym. Mater. Sci. Eng.* **1999**, *80*, 68.

(8) (a) Wu, D.; Chen, A.; Johnson, C. S., Jr. *J. Magn. Res.* **1995**, *A115*, 260. (b) Gibbs, S. J.; Johnson, C. S., Jr. *J. Magn. Res.* **1991**, *93*, 395.

(9) Lakowicz, J. R. *Topics in Fluorescence Spectroscopy*; Plenum Press: New York, 1991; Vol.1 & 2.

(10) (a) Hawker, C. J.; Frechet, J. M. J. *J. Am. Chem. Soc.* **1990**, *112*, 7638. (b) Seebach, D.; Lapierre, J.-M.; Greiveldinger, G.; Skobridis, K. *Helv. Chim. Acta* **1994**, *77*, 1673. (c) Furniss, B. S.; Hannaford, A. J.; Rogers, V.; Smith, P. W. G.; Tatchell, A. R. *Vogel's Textbook of Practical Organic Chemistry,* 4th ed.; John Wiley & Sons: New York: 1978, p 841.

(11) Furniss, B. S.; Hannaford, A. J.; Rogers, V.; Smith, P. W. G.; Tatchell, A. R. *Vogel's Textbook of Practical Organic Chemistry,* 4th ed.; John Wiley & Sons: New York: 1978, p 754.

(12) (a) Brown, H. C.; Narasimhan, S.; Choi, Y. M. *J. Org. Chem.* **1982**, *47*, 4702. (b) Tyler, T. L.; Hanson, J. E. *Chem. Mater.* **1999**, *11*, 3452.

(13) Sehgal, R. K.; Kumar, S. *Org. Prep. Proced. Int.* **1989**, *21*, 223.

(14) Rodenburg, L.; Floor, M.; Lefeber, A.; Cornelisse, J.; Lugtenburg, J.; *Recl. Trav. Chim. Pays-Bas* **1988**, *107*, 1.

(15) Schofield, E.; Schulz R. C. *Makromol. Chem., Rapid Commun.* **1981**, *2*, 677.

(16) Wooley, K. L.; Hawker, C. J.; Frechet, J. M. J. *J. Am. Chem. Soc.* **1993**, *115*, 11496.

(17) (a) Pysh, E. S.; Yang, N. C. *J. Am. Chem. Soc.* **1963**, *85*, 2124. (b) Mann, C. K.; Barnes K. K. *Electrochemical Reactions in Nonaqueous Systems*; Marcel Dekker, Inc.: New York, 1970.

(18) (a) Riley, J. M. Synthesis, Characterization, and Photophysical Studies of Poly(aryl ether) Monodendrons and Pyrene Labeled Poly(aryl ether) Monodendrons. Ph.D. Dissertation, Seton Hall University, 1998. (b) Khan, W. A. Pyrene Labeled Poly(aryl ether) Monodendrons: Synthesis and Photophysical Studies. Ph.D. Dissertation, Seton Hall University, 1999.

(19) (a) Turro, N. J.; Barton, J. K.; Tomalia, D. A. *Acc. Chem. Res.* **1991**, *24*, 332. (b) Kalyanasundaram, K. *Photochemistry in Microheterogeneous Systems*; Academic Press: New York, 1987.

(20) (a) Birks, J. B., Ed. *Organic Molecular Photophysics*; John Wiley and Sons: New York, 1973. (b) Murov, S. L.; Carmichael, I.; Hug, G. L. *Handbook of Photochemistry,* 2nd ed.; Marce Dekker: New York, 1993.

(21) (a) Ware, W. R. *J. Phys. Chem.* **1962**, *66*, 455. (b) Kawaoka, K.; Khan, A. U.; Kearns, D. R. *J. Chem. Phys.* **1967**, *46*, 1842. (c) Parmenter, C. S.; Rau, J. D. *J. Chem. Phys.* **1969**, *51*, 2242. (d) Potashnik, R.; Goldschmidt, C. R.; Ottolenghi, M. *Chem. Phys. Lett.* **1971**, *9*, 424. (e) Watkins, A. R. *Chem. Phys. Lett.* **1979**, *65*, 380.

(22) (a) Patterson, L. K.; Porter, G.; Topp, M. R. *Chem. Phys. Lett.* **1970**, *7*, 612. (b) Vaughan, W. M.; Weber, G. *Biochemistry* **1970**, *9*, 464. (c) Olea, A. F.; Thomas, J. K. *J. Am. Chem. Soc.* **1988**, *110*, 4494.

(23) (a) Bohorquez, M.; Patterson, L. K. *Langmuir* **1990**, *6*, 1739. (b) Fischkoff, S.; Vanderkooi, J. M. *J. Gen. Physiol.* **1975**, *65*, 663.

(24) (a) Stern, O.; Volmer, M. *Phys. Z.* **1919**, *20*, 183. (b) Barltrop, J. A.; Coyle, J. D. *Principles of Photochemistry*; John Wiley and Sons: New York, 1978. (c) Turro, N. J. *Modern Molecular Photochemistry*; University Science Books: Mill Valley, CA, 1991. (d) Green, N. J. B.; Pimblott, S. M.; Tachiya, M. *J. Phys. Chem.* **1993**, *97*, 196.

(25) Stejskl, E. O.; Tanner, J. E. *J. Chem. Phys.* **1965**, *42*, 288.

(26) Berlman, I. B. *Handbook of Fluorescence Spectra of Aromatic Molecules*; Academic Press: New York, 1965.

(27) (a) Tyrrell, H. J. V. *Diffusion and Heat Flow in Liquids*; Butterworths: London, 1961. (b) Ricka, J.; Gysel, H.; Schneider, J.; Nyffenegger, R.; Binkert, T. *Macromolecules* **1987**, *20*, 1407.

(28) (a) Rabinovich, L. B. *The Influence of Isotopy on the Physico-Chemical Properties of Liquids*; Consultants Bureau: New York, 1970. (b) Cataliotti, R. S.; Sassi, P.; Morresi, A.; Paliani, G. *Chem. Phys.* **2000**, *255*, 85.

(29) Fully extended radii were measured from Dreiding models, which gave a distance of 5.8 Å across a single monomer unit. As a rough approximation, half of this value should be the increase in the radius for each generation, the generational radial increment. This results in an increment of 2.9 Å per generation. The baseline radius of 7.2 Å for G0Py was estimated from the radius of pyrene and a benzyloxy group. See ref 28a.

(30) (a) Flory, P. J. *J. Chem. Phys.* **1949**, *17*, 303. (b) Flory, P. J. *Principles of Polymer Chemistry*; Cornell University Press: Ithaca, NY, 1971. (c) Flory, P. J. *Polymer Science*: *Achievements and Prospects*; Markovitz H., Casassa, E. F., Eds.; Wiley-Interscience: New York, 1976. (d) de Gennes, P. G. *Scaling Concepts in Polymer Physics*; Cornell University Press: Ithaca, NY, 1979. (e) Gedde, U. W. *Polymer Physics*; Chapman and Hall: New York, 1995. (f) Schafer, L. *Excluded Volume Effects in Polymer Solutions*; Springer-Verlag: Berlin, 1999.

(31) Edward, J. T. *J. Chem. Educ.* **1970**, *47*, 261.

(32) Bondi, A. *J. Phys. Chem.* **1964**, *68*, 441.

(33) (a) Smoluchowski, M. V. *Z. Phys. Chem.* **1917**, *92*, 129. (b) Sveshnikoff, B. *Acta Physicochem. USSR* **1949**, *3*, 257. (c) Nemzek, T. L.; Ware, W. R. *J. Chem. Phys.* **1975**, *62*, 477. (d) Keizer, J. *Chem. Rev.* **1987**, *87*, 167. (e) Lakowicz, J. R.; Joshi, N. B.; Johnson, M. L.; Szmacinski, H.; Gryczynski, I. *J. Biol. Chem.* **1987**, *262*, 10907.

(34) (a) Szabo, A.; Shoup, D.; Northrup, S. H.; McCammon, J. A. *J. Chem. Phys.* **1982**, *77*, 4484. (b) Northrup, S. H.; McCammon, J. A. *J. Am. Chem. Soc.* **1984**, *106*, 930. (c) Barboy, N.; Feitelson, J. *Biochemistry* **1987**, *26*, 3240. (d) Caldin, E. F.; Queen, A. *Reactions in Compartmentalized Liquids*; Knoche, W., Schomacker, R., Eds. Springer-Verlag: Berlin, 1989.

(35) The model is constructed in two dimensions as follows. Consider two circles, smaller circle C1 with radius R and larger circle C2 with radius R', touching at a single point. A right triangle can be constructed from three lines: a line connecting the centers of the two circles, with length $R + R'$ (this is the hypotenuse); a line from the center of C1 that is tangent to C2; and a line from the point of tangency to the center of C2. The angle ϕ at the center of circle C1 is such that $\sin \phi = R'/(R + R')$, or $\phi = \sin^{-1}(R'/(R + R'))$. The arc on C1 within the triangle is equal to ϕR, with ϕ in radians. The total length occluded is twice this value, $2\phi R$. The fraction occluded is the length occluded ($2\phi R$) divided by the total circumference, $2\pi R$. A simple expression for this is ϕ/π. To extend this model to three dimensions, rotation of the two circles about the line joining their centers will define two spheres, S1 and S2. These spheres contain an infinite number of circles with this same relationship; therefore the surface area of S1 occluded by S2 should also be ϕ/π.

(36) *CRC Handbook of Chemistry and Physics,* 78th ed.; Lide, D. R., Ed. CRC Press: Boca Raton, FL, 1997.

MA0007886